

# Modulation of physical properties of oxide thin films by multiple fields\*

Huali Yang(杨华礼)<sup>1,2</sup>, Baomin Wang(王保敏)<sup>1,2,†</sup>, Xiaojian Zhu(朱小健)<sup>1,2</sup>,  
Jie Shang(尚杰)<sup>1,2</sup>, Bin Chen(陈斌)<sup>1,2</sup>, and Runwei Li(李润伟)<sup>1,2,‡</sup>

<sup>1</sup>Key Laboratory of Magnetic Materials and Devices, Ningbo Institute of Materials Technology and Engineering, Chinese Academy of Sciences, Ningbo 315201, China

<sup>2</sup>Laboratory of Magnetic Materials and Application Technology, Ningbo Institute of Materials Technology and Engineering, Chinese Academy of Sciences, Ningbo 315201, China

(Received 17 March 2015; revised manuscript received 4 May 2015; published online 20 April 2016)

Recent studies of the modulation of physical properties in oxide thin films by multiple fields are reviewed. Some of the key issues and prospects of this area of study are also addressed. Oxide thin films exhibit versatile physical properties such as magnetism, ferroelectricity, piezoelectricity, metal–insulator transition (MIT), multiferroicity, colossal magnetoresistivity, switchable resistivity. More importantly, the exhibited multifunctionality can be tuned by various external fields, which has enabled demonstration of novel electronic devices.

**Keywords:** multiple fields, functional oxides, thin film

**PACS:** 73.23.–b, 73.50.Pz, 77.55.Nv

**DOI:** 10.1088/1674-1056/25/6/067303

## 1. Introduction

Oxides are a class of materials that are particularly attractive due to their remarkable physical properties and multifunctionality.<sup>[1–4]</sup> For example, a diversity of physical properties exhibited in thin film oxides, such as magnetism, ferroelectricity, piezoelectricity, and superconductivity, have been intensively studied in the past several decades,<sup>[5–10]</sup> and the interplay between them has become a hot topic in condensed matter physics.<sup>[11–15]</sup> Intriguing phenomena including MIT,<sup>[16–24]</sup> colossal magnetoresistivity,<sup>[25–29]</sup> resistive switching,<sup>[30–38]</sup> ferroelectricity,<sup>[39–45]</sup> multiferroicity,<sup>[46–56]</sup> etc., make oxides appealing candidates for both electronic and spintronic devices.<sup>[57–63]</sup> From a fundamental perspective, the multifunctionality in oxides provides a playground for investigating the interplay between spin, charge, orbital and lattice degrees of freedom.<sup>[24,64–67]</sup> A number of interesting phenomena such as charge order, orbital order, multiferroicity, and interactions such as the electron correlation effect, Jahn–Teller interaction, and spin-orbit coupling, have been frequently discussed to understand the fundamental physics.<sup>[51,64,68–73]</sup> In addition, the advent of atomically tailored oxide heterostructures has enabled the observation of emergent phenomena, and raised excitement in the study of novel phenomena due to the symmetry breaking and charge transfer across the oxide

interface.<sup>[67,73–76]</sup>

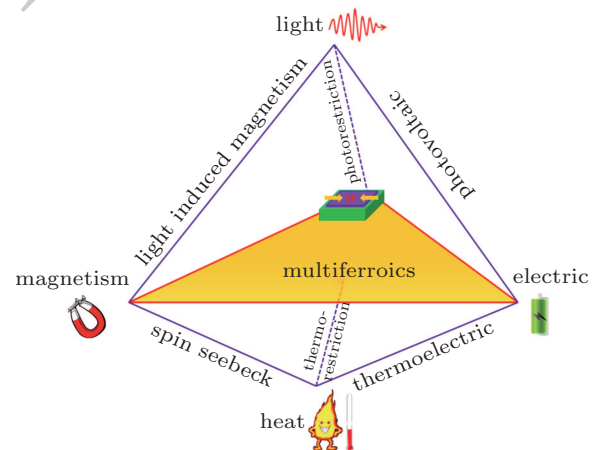


**Fig. 1.** Schematic showing the various fields (light, magnetism, heat, electric, and strain) modulating the physical properties in oxides.

The interplay between spin, charge, orbital, and lattice degrees of freedom in oxides (especially complex oxides) reveals strong composition–structure–property relationships, and it enables study of the effects of various types of fields in various combinations on the physical properties of thin film oxides. As shown in Fig. 1, the interconnections between light, magnetism, heat, strain, and electric has been demonstrated in condensed matters, and many novel phenomena such as

\*Project supported by the State Key Project of Fundamental Research of China (Grant No. 2012CB933004), the National Natural Science Foundation of China (Grant Nos. 11274321, 51301191, 61328402, and 11274322), Overseas, Hong Kong & Macao Scholars Collaborated Researching Fund (Grant No. 51428201), the Instrument Developing Project of the Chinese Academy of Sciences (Grant No. YZ201327), Ningbo Major Project for Science and Technology (Grant No. 2014B11011), and Ningbo International Cooperation Projects (Grant No. 2012D10018).

†Corresponding author. E-mail: wangbaomin@nimte.ac.cn

‡Corresponding author. E-mail: runweili@nimte.ac.cn

photostriction,<sup>[77]</sup> thermal spin-transfer torque,<sup>[78]</sup> and multiferroicity have been revealed in functional oxides. Many novel devices with multifunctionality have been proposed, such as spin-resistive random access memories (RRAM), electric operational magnetic random access memories (MRAM), multiferroic tunnel junctions, etc.

In many cases, combined external stimuli could enable fine tuning of physical properties in thin film oxides, which could benefit practical applications. In the following paragraphs, we will discuss the response of thin film oxides to an external stimulus such as electrical field, strain field, magnetic field or photo illumination. We have focused special concern on multiferroics, perovskite manganites, and oxides with resistive switching (RS) properties.

## 2. Electric field effect

Electric field has been recognized as an efficient and scalable way to tune the physical properties in various materials and structures. For example, in magnetic tunneling junctions, a spin polarized current can induce spin transfer torque effect, which has been intensively studied in MRAM devices<sup>[79–82]</sup> and microwave devices.<sup>[83]</sup> Upon the application of electric field, the polarization direction of ferroelectrics can be switched. This can result in either a large electroresistance effect in ferroelectric tunnel junctions<sup>[84,85]</sup> or a switchable diode effect in ferroelectric diodes.<sup>[86]</sup> Noticeable strain effect associated with electric-field-induced ferroelastic domain switching has also been intensively studied in magnetoelectric heterostructures.<sup>[87,88]</sup> In multiferroic materials where the electric polarization couples with the magnetization, applying an electric field modifies the electric polarization and tunes its magnetization through the magnetoelectrical (ME) coupling effect.<sup>[11,89,90]</sup> In RRAM devices, applying an electric field induces the RS effect by associating with several electric-field-induced effects: electric field induced ion transport,<sup>[35]</sup> electric field induced phase transition,<sup>[91]</sup> and the Joule heating effect.<sup>[92]</sup>

### 2.1. Electric field control of magnetism

The interplay between electric polarization and magnetization has attracted wide interest for applications such as spintronic devices.<sup>[48,93]</sup> The presence of multiferroicity in some materials and structures has enabled several ways for the magnetic properties to be manipulated by applying an electric field:<sup>[94]</sup> (i) In single phase multiferroics where magnetic order and ferroelectricity are coupled, applying an electric field can alter the electric polarization along with the magnetization, owing to intrinsic ME coupling.<sup>[11]</sup> (ii) Many multiferroics are antiferromagnets; by attaching a multiferroic layer to a ferromagnetic layer, it is possible to construct an exchange bias sys-

tem that can be controlled by applying electric field to the multiferroic layer, which is known as exchange-mediated ME coupling effect.<sup>[12]</sup> (iii) In magnetoelectric composites composed of ferroelectric (FE)/ferromagnetic (FM) heterostructures,<sup>[95]</sup> applying an electric field in the FE layer induces strain that is transmitted in to the FM layer and changes its magnetic properties through inverse magnetostrictive effect. (iv) In FE/FM heterostructures, the electric field can also switch the polarization direction of the FE layer, which may tune the carrier density and hence the magnetic properties of the FM layer, a phenomenon called charge-mediated ME coupling effect.<sup>[96]</sup>

In single phase multiferroic materials, a tempting idea is to design multiferroics that combine both ferromagnetism and ferroelectricity, and the manipulation of its magnetization by an electric field would be essential for the magnetoelectric control of spintronic devices. However, the exploration of ferromagnetism and ferroelectricity together in a single phase multiferroic has been found unexpectedly difficult.<sup>[46]</sup> One promising single phase multiferroic that could be utilized is BiFeO<sub>3</sub> (BFO) — a material that unambiguously shows ferroelectricity and anti-ferromagnetism above room temperature.<sup>[97]</sup> The principle that BFO can be utilized for efficient magnetoelectric control of spintronic devices relies on the possibility of electric field controlled interfacial coupling composed of a BFO layer and a ferromagnetic layer.<sup>[12,98,99]</sup>

Recently, Heron *et al.* demonstrated deterministic magnetization reversal in BFO based heterostructures,<sup>[99]</sup> by utilizing the coupling between its weak magnetization arising from the Dzyaloshinskii–Moriya (DM) interaction and the ferroelectric polarization,<sup>[100,101]</sup> as well as the strong interfacial magnetic coupling.<sup>[102]</sup> Earlier, theory had predicted<sup>[103]</sup> that the direct reversal of ferroelectric polarization in BFO will leave the orientation of the canted magnetic moment unchanged, Heron *et al.* found that ferroelectric-polarization reversal in a strained BFO film actually follows an indirect pathway, and proposed that the indirect switching path reverses the canted magnetic moment [Fig. 2]. The ME coupling is determined by the DM interaction, where the weak ferromagnetism  $M_c$  is determined by the DM vector given by  $\mathbf{D} \sim \sum \mathbf{d}_i \times \mathbf{r}_i$ , where  $\mathbf{r}_i$  is a constant vector that connects neighboring Fe<sup>3+</sup> ions and  $\mathbf{d}_i$  is the displacement of the intermediate oxygen atom from the mid-point of  $\mathbf{r}_i$  caused by the O<sub>6</sub>-rotation. Since the in-plane 71° and out-of-plane 109° switches are found to be capable of rotating  $\mathbf{D}$  and the associated  $M_c$  by 90° [Figs. 2(b) and 2(c)], the reversal of  $\mathbf{D}$  through the sequential in-plane 71° and out-of-plane 109° switches would also be expected to reverse  $M_c$ . Furthermore, they deposited a spin valve structure on top of the strained BFO and realized the electric-field control of a spin-valve device at room temperature.

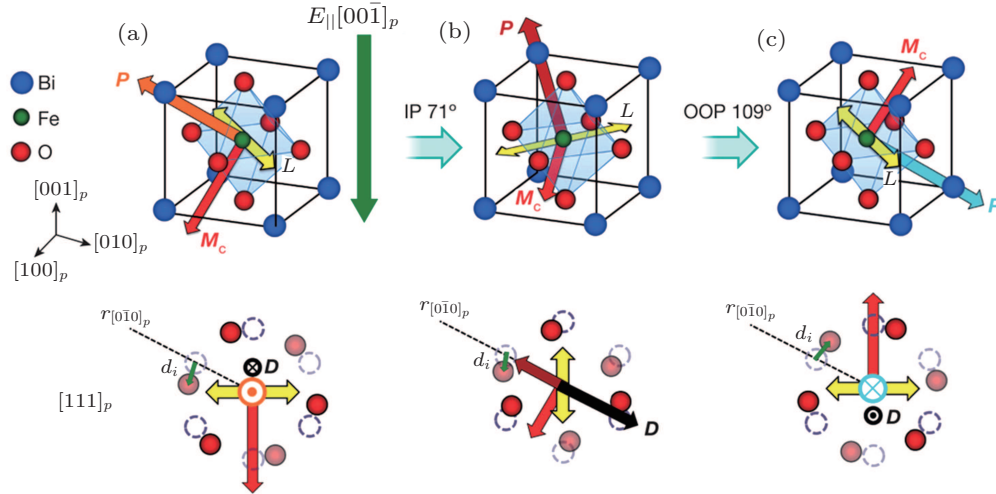


**Fig. 2.** (a) A domain with polarization  $P$  initially along the  $(1\bar{1}1)$ .  $L$  represents the antiferromagnetic axis.  $O_6$  rotations are shown with respect to an octahedron that is not rotated (dashed circles). (b) After an in-plane  $71^\circ$  switch.  $E$  represents the applied electric field. (c) After an out-of-plane  $109^\circ$  switch.<sup>[99]</sup>

Progress in strain-mediated and charge-mediated ME effect will be further discussed in later sections.

**2.2. Electric field induced ion migration**

RRAM has been widely investigated for next-generation nonvolatile memory devices due to its simple structure, high density, low power consumption and compatibility with complementary metal oxide semiconductor technology.<sup>[61,104–106]</sup>

Up to now, a large variety of materials have been investigated for RS, including solid electrolytes,<sup>[107]</sup> perovskite oxides,<sup>[32,108–110]</sup> binary oxides,<sup>[33,35,37,111]</sup> organic materials,<sup>[112–114]</sup> amorphous silicon,<sup>[115]</sup> and amorphous carbon.<sup>[116]</sup> Although the underlying mechanism is still controversial due to the diversity of RS behaviors, the conductive filament (CF) model has gained much success and has been accepted extensively.<sup>[34]</sup>

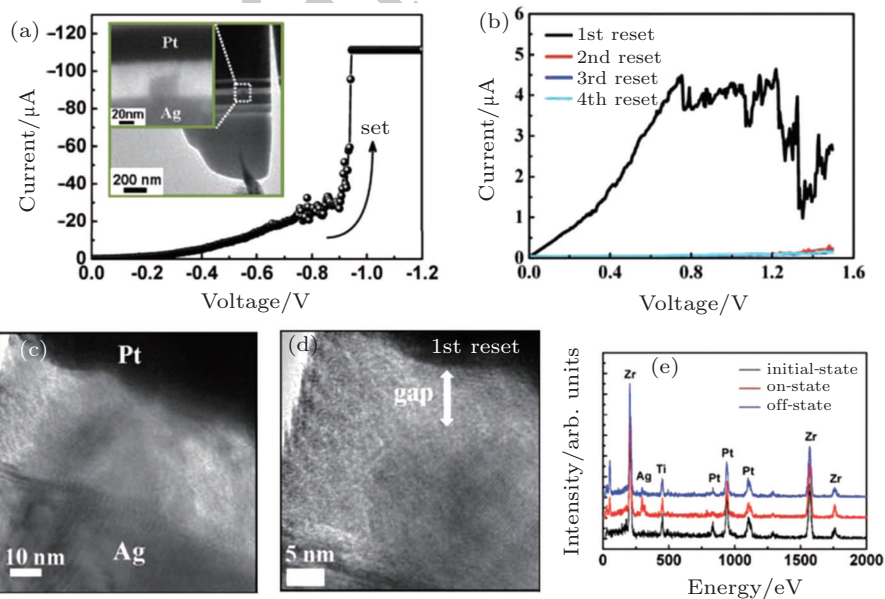


**Fig. 3.** (a)  $I$ - $V$  curve of the  $Ag/ZrO_2/Pt$  TEM specimen during SET operation. Inset is a TEM image of the specimen after the SET process. (b)  $I$ - $V$  curves of the TEM specimen under successive RESET operations. (c) High resolution TEM image of the CF region in an  $Ag/ZrO_2/Pt$  TEM specimen after SET process. (d) High resolution TEM images showing that the CF dissolves from the anode (Pt) to the cathode (Ag) terminal during RESET voltage sweeps ( $0 \rightarrow 1.5$  V). (e) EDX analysis of the TEM specimen conducted at the initial-, ON- and OFF-states.<sup>[36]</sup>

RRAM devices have a simple metal-insulator-metal sandwiched structure. For filament model based RRAMs, a sufficiently large electrical field between the two metallic electrodes can induce a soft dielectric breakdown in the insulator and set the device to a conductive state (also called an ON-state). In this process, due to the electrically induced

ion migration, a large number of defects are formed inside the film and form CFs that connect the two terminal electrodes. The ON-state can also be electrically reset, leading to the OFF-state that corresponds to disruption of the CFs. In the CF model, the formation and rupture of local conducting paths connecting the two-terminal electrodes domi-

nates the RS process.<sup>[36,38,117,118]</sup> Liu *et al.* have performed real-time characterizations of the CF formation and dissolution processes of an oxide-electrolyte-based RRAM device<sup>[36]</sup> that is based on a vertical Ag(Cu)/ZrO<sub>2</sub>/Pt structure with both small lateral sizes and ZrO<sub>2</sub> thickness to facilitate direct TEM studies. During the SET process, a dark nano-bridge region appears, signifying the formation of CF [Fig. 3(a)]. Successive RESET process has been performed, and a first RESET voltage sweep is found to decrease the electrical current passing through the device drastically [Fig. 3(b)]. Meanwhile, the CF region near the Pt electrode was substantially weakened after the first RESET process [Fig. 3(c) and 3(d)]. The chemical compositions of the CF region in the initial-, ON- and OFF-states were analyzed using energy-dispersive x-ray spectroscopy (EDX) analysis and are found to be Ag in the Ag/ZrO<sub>2</sub>/Pt device [Fig. 3(e)]. These experiments have led to

intuitive, more complete understanding of the underlying nature of the RS behavior and the corresponding CF evolution process.

It has been found that the nanoscale conduction channel not only dominates the RS process but also shows some other effects, such as quantum size effects and exchange bias effect. For example, quantized conductance has been realized in zinc-oxide based sandwich devices.<sup>[35]</sup> As can be seen from Fig. 4, the Nb/ZnO/Pt device shown in Fig. 4(a) can be Set and Reset repeatedly, exhibiting typical bipolar RS behaviors [Fig. 4(b)]. During the Set process where the nanoscale conducting channel is forming, the conductance shows quantum behavior corresponding to electron travelling along the nanoscale channel [Fig. 4(c) and (d)]. Similar phenomena have also been found in other sandwiched thin films.<sup>[118–122]</sup>

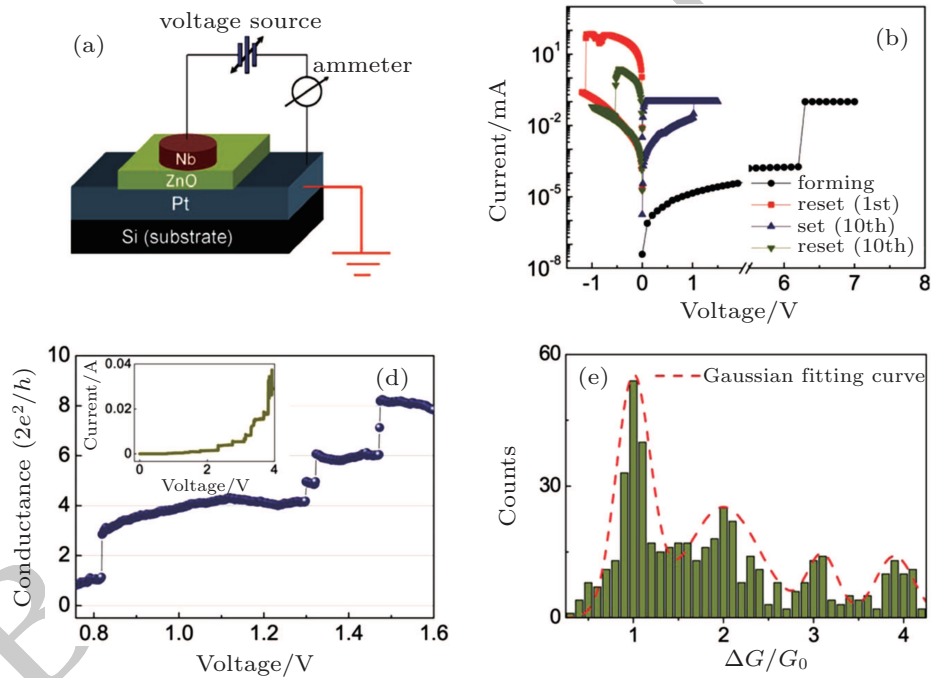


**Fig. 4.** (a) Schematic of a sandwiched Nb/ZnO/Pt structure. (b) Typical bipolar RS behaviors observed in the device. (c) Measured conductance as a function of the bias voltage during the set process. Inset: Corresponding  $I$ - $V$  curve in a larger voltage range from 0 V to 4 V. (d) Histogram of the conductance changes  $\Delta G$  obtained from the forming and set processes.<sup>[35]</sup>

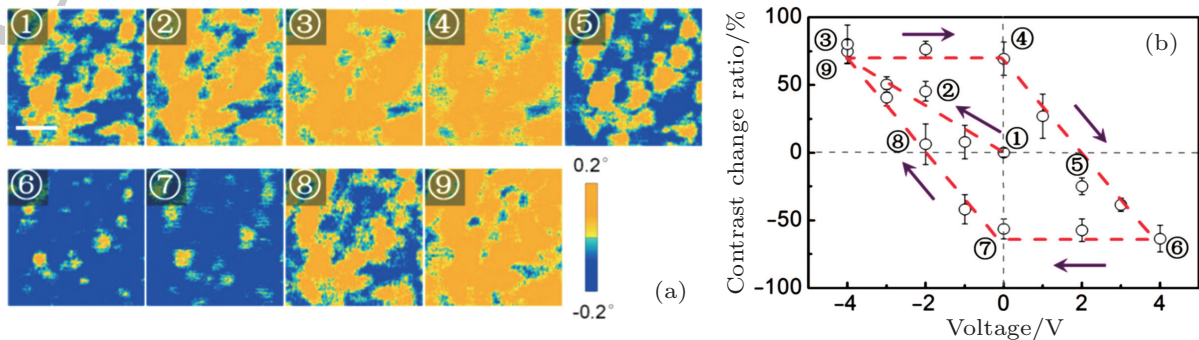


**Fig. 5.** (a) MFM images of the CFO thin film at the pristine state and after being subjected to various bias voltages. The scale bar is 200 nm. (b) Evolution of the contrast change ratio (defined as the ratio between the total areas of the electrically-produced upward-magnetized domains and the initially upward-magnetized domains) after being subjected to various biased voltages in the sequence of 0 V  $\rightarrow$  -4 V  $\rightarrow$  0 V  $\rightarrow$  4 V  $\rightarrow$  0 V  $\rightarrow$  -4 V.<sup>[126]</sup>

It has also been revealed that by controlling the migration of ions through electrical fields, the magnetism of some magnetic dielectrics can be modulated. For example, Chen *et al.* successfully modulated the magnetization and coercive field of Co-doped ZnO thin films.<sup>[123]</sup> Similar behavior has been reported in other materials such as Mn:ZnO<sup>[124]</sup> and Fe<sub>3</sub>O<sub>4</sub>.<sup>[125]</sup> In CoFe<sub>2</sub>O<sub>4</sub> (CFO) thin films, nanoscale magnetization reversal *via* electrical ion-manipulation at room temperature has been reported.<sup>[126]</sup> As is shown in Fig. 5(a), after being subjected to various bias voltages, the MFM signal of CFO thin films indicates magnetization reversal. The electric field modulates the magnetization in CFO thin films in a reversible and non-volatile manner [Fig. 5(b)], and can be realized without the assistance of external magnetic field. This strategy of utilizing electric field-induced migration and redistribution of ionic species to modulate the nanoscale magnetization is favorable for the construction of novel spintronic devices.

### 2.3. Electric field induced MIT

In thin film oxides, besides the ionic transport process, the RS phenomenon is associated with other mechanisms such as self-Joule heating effect<sup>[92]</sup> and electric field induced electronic phase transition.<sup>[91]</sup> The electric field induced electronic phase transition has been predicted theoretically in charge-orbital ordered manganites, where applying an electric field may suppress the charge ordering and drive the system from the antiferromagnetic charge-ordered state to the ferromagnetic metallic state, resulting in the well-known MIT.<sup>[127]</sup> The electric field induced magnetism in manganites is a newly found way of realizing the electrical control over magnetism.<sup>[128,129]</sup> Another very interesting and widely studied correlated material with electric field induced MIT is vanadium dioxide (VO<sub>2</sub>). Bulk VO<sub>2</sub> exhibits MIT at temperature  $\sim 340$  K.<sup>[130]</sup> The electric field was found to be able to drive MIT in VO<sub>2</sub>, accompanied by a structural change<sup>[131]</sup> and a large isothermal entropy change.<sup>[132]</sup> Various electronic devices have been proposed based on the electric field induced MIT in VO<sub>2</sub>.<sup>[133,134]</sup> However, the underlying mechanisms have not been fully clarified.<sup>[135–138]</sup>

### 2.4. Electrical modulation of the carrier density

The electronic structures of some functional oxides (such as manganites) depend critically on the doping level; hence doping enables electrostatic field tuning of their physical properties.<sup>[139,140]</sup> The charge-mediated tuning of functionality (such as electron transport and magnetization) in oxides has been studied both theoretically<sup>[141–144]</sup> and experimentally<sup>[96,145,146]</sup> in a number of heterostructures.

In perovskite manganites, the electrostatic field can modify the charge carrier concentration without affecting the lattice distortion, which is useful to study the influence of band filling on the electronic properties. The only challenge comes from the high carrier concentration in FM manganites (with carrier density as high as  $10^{21}$  carriers per cm<sup>3</sup>), which results in an electronic screening length on the order of only 1 nm (the Thomas–Fermi screening limit), limiting the tun-

ability of the electrostatic field imposed by utilizing conventional dielectrics, like SiO<sub>2</sub>, SrTiO<sub>3</sub> (STO), and ferroelectrics such as lead zirconate titanate (PZT).<sup>[140,147]</sup> In recent years, the electric double-layer transistor (EDLT) has been used to achieve high electric fields, enabling charge accumulation in the channel surface at densities as high as  $10^{15}$  per cm<sup>2</sup>.<sup>[148]</sup> This is almost two orders of magnitude larger than that in conventional field effect transistors, thus providing better access to electrostatic modulation of electronic phases. The effective tunability by using EDLT has been demonstrated in manganite transistors such as (La, Ca)MnO<sub>3</sub> (LCMO) transistors,<sup>[149]</sup> (Pr,Sr)MnO<sub>3</sub> (PSMO) thin films,<sup>[150]</sup> and (Pr,Ca,Sr)MnO<sub>3</sub> (PCSMO) thin films.<sup>[151]</sup> For example, in PCSMO thin films, it is found that, consistent with the phase diagram, electrostatic modulation of the carrier concentration can effectively modify the phase transition temperature. Electrostatic modulation can also co-play with external magnetic field, resulting in the fine tuning of electronic phase and phase transitions.<sup>[150,151]</sup>

An MIT can be induced by a gating field in VO<sub>2</sub>, and the electrostatic effect caused by the gating field was found by Nakano *et al.* to overcome the Thomas–Fermi screening limit.<sup>[152]</sup> They suggested that the Thomas–Fermi screening limit does not apply to materials such as VO<sub>2</sub>, which is characterized by inherent collective interactions between electrons and the crystal lattice. Jeong *et al.*,<sup>[153]</sup> however, showed that the electrolyte gating of VO<sub>2</sub> leads not to electrostatically induced carriers but instead to the electric field induced creation of oxygen vacancies. They found that by sweeping  $V_G$ , the device can be reversibly switched between the insulating and metallic states. Hysteresis in the sheet conductance centered about  $V_G = 0$  V was observed [Fig. 6(a)], and the high conductance state was maintained for many days even when the ionic liquids were washed off. XPS was taken to measure changes in the oxidation state of vanadium in VO<sub>2</sub> films, and they have observed a reduction in the oxidation state of V from V<sup>4+</sup> toward V<sup>3+</sup> when the film is gated [Fig. 6(b)], indicating migration of oxygen from the oxide film into the ionic liquid. These results are consistent with the correlation between the source-drain current and the amount of oxygen pressure [Fig. 6(c)].

The mechanism associated with electric field induced oxygen migration has also been suggested by Cui *et al.*<sup>[154,155]</sup> in ionic liquid gating experiments on (La,Sr)MnO<sub>3</sub> (LSMO). Although oxygen vacancy migration has not been directly observed, the Mn valence variation in XPS and microstructure evolution in HRTEM under different gate voltages suggest the formation and annihilation of oxygen vacancies. The electric fields created by the electric double layer (EDL) on a manganite under  $V_G$  will change the chemical composition, which is accompanied by changes in the effective doping level  $x$  [Fig. 7(a)]. Interestingly, an effective tuning of the orbital occupancy and corresponding magnetic anisotropy by gate voltage have been observed by using x-ray linear dichroism (XLD) [Fig. 7(b) and 7(c)]. The tuning behaves in a reversible and quantitative manner, manifesting advances towards practical oxide-electronics based on orbital.

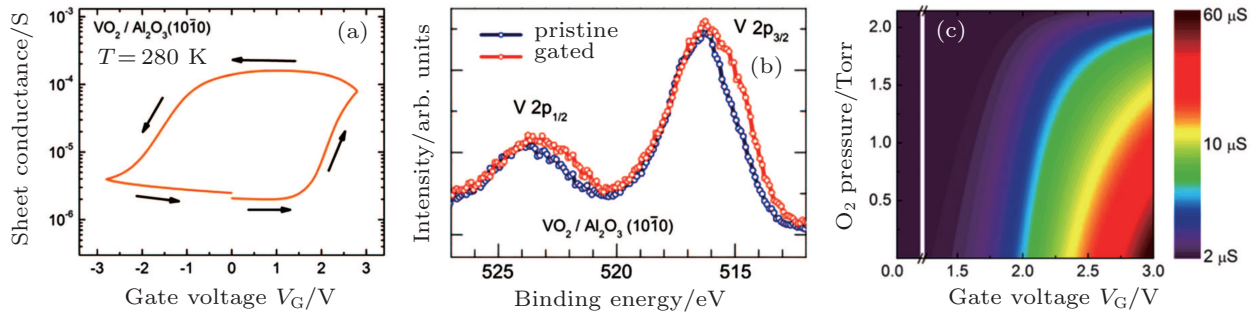


**Fig. 6.** (a) Sheet conductance versus  $V_G$  for devices fabricated from  $\text{VO}_2$  films prepared on  $\text{Al}_2\text{O}_3(10\bar{1}0)$ . (b) V 2p core-level spectra for pristine and gated  $\text{VO}_2/\text{Al}_2\text{O}_3(10\bar{1}0)$  at  $V_G = 1.8$  V. (c) Sheet conductance (color scale) as a function of  $V_G$  and  $\text{O}_2$  pressure.<sup>[153]</sup>

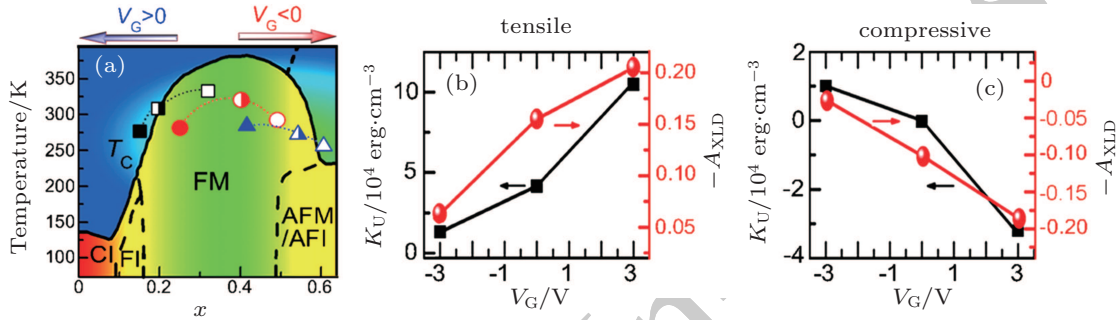


**Fig. 7.** (a) Electronic phase diagram of LSMO with varying  $x = \text{Mn}^{4+}/(\text{Mn}^{3+} + \text{Mn}^{4+})$  ratio. The half-filled triangle, circle, and square denote the positions of samples on STO with initial  $x = 0.54, 0.41,$  and  $0.20$  in phase diagram, respectively. The sample positions after applying positive and negative  $V_G$  are marked by corresponding filled and empty symbols. The abbreviations stand for spin-canted insulating (CI), ferromagnetic insulating (FI), ferromagnetic metal (FM), antiferromagnetic metal (AFM), and antiferromagnetic insulating (AFI) phase, respectively. The dependence of  $K_U$  (left axis) and  $-A_{\text{XLD}}$  (right axis) on  $V_G$  for the case of (b) tensile and (c) compressive strain.<sup>[155]</sup> The unit  $1 \text{ erg} = 10^{-7} \text{ J}$ .

### 3. Strain effect

Applying strain on thin film oxides has been proven to be an efficient way for tuning their physical properties. Exerting strain on thin films can induce distortions of the film unit cell, which changes the elastic energy and modifies the films' electro-magnetic properties.<sup>[156]</sup> In some cases, applying strain can alter the ground state of thin film oxides and novel phases are disclosed. There are three ways to apply strain in thin films: mechanical strain,<sup>[157]</sup> epitaxial strain,<sup>[158]</sup> and strain that is due to the converse piezoelectric effect.<sup>[159]</sup> In recent years, inspired by the idea of wearable electronic devices, there has been increasing interest in the study of flexible electronic devices,<sup>[160–164]</sup> and the strain effect in these devices has been intensively investigated.

#### 3.1. Strain tuning of the electronic phases

In some transition metal oxides, the electronic phases are very sensitive to external strain,<sup>[165,166]</sup> resulting in highly sensitive electrical and magnetic response to external strain field. For example, the strain effect on the electrical properties of manganite thin films has been studied by using the converse piezoelectric effect; the resistance of manganite thin films is found to change dramatically under small strain, resulting in very large strain gauge factor.<sup>[159,167–169]</sup> The electrical and magnetic response to external strain is essentially

mediated by the piezostrain coupled orbital reoccupation<sup>[170]</sup> and electronic phase separation.<sup>[169]</sup> Zheng *et al.* investigated the influences of piezostrain on the electronic transport and magnetic properties of charge-ordered  $\text{La}_{0.5}\text{Ca}_{0.5}\text{MnO}_3$  thin films.<sup>[169]</sup> An unprecedented large strain-induced resistance change is found to be magnetic-field tunable [Fig. 8(a)], indicating that this coupling is essentially mediated by the electronic phase separation. By using the ferroelastic domain switching of the ferroelectric substrate [Figs. 8(c) and 8(d)],

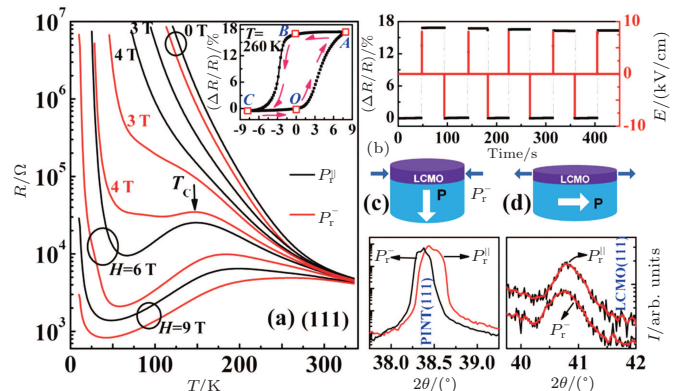


**Fig. 8.** (a) Temperature dependence of resistance for the LCMO (111) film in the magnetic fields as stated when the ferroelectric substrate was in the  $P_r^{\parallel}$  and  $P_r^{-}$  states, respectively. Inset in panel (a):  $\Delta R/R$  of the film as a function of  $E$  at  $T = 260$  K. (b) Nonvolatile resistance switching of the LCMO film by a pulsed electric field at  $T = 260$  K. (c) and (d) Schematics of the ferroelastic strain effect at  $T = 260$  K. (e) and (f) XRD  $\theta$ - $2\theta$  scans for the ferroelectric substrate and LCMO film when the ferroelectric substrate was in the  $P_r^{\parallel}$  and  $P_r^{-}$  states, respectively.<sup>[169]</sup>

they found that an in-plane tensile strain (correspond to the  $P_r^-$  state) as small as 0.1% according to x-ray diffraction [Fig. 8(e) and 8(f)] can induce a large increase in the resistance and  $T_{CO}$  and a drop in magnetoresistance, signaling the stabilizing of the charge-ordered phase. On the other hand, an in-plane compressive strain (correspond to the state) suppresses the charge-ordered phase. By taking advantage of the ferroelastic strain, electric-field-controlled non-volatile RS behavior can be achieved [inset of Fig. 8(a) and Fig. 8(b)]. Besides the large strain-induced resistivity change, applying anisotropic strain field is found to induce highly anisotropic resistivity in perovskite manganites.<sup>[171,172]</sup>

The substrate strain can sometimes induce new phases with dramatic electron transport properties. For example, it has been predicted theoretically that in a half-doped manganite, the ferromagnetic charge ordered insulating state, pre-

viously inaccessible to experiments, becomes stable under tensile strain.<sup>[173]</sup> A recent report on LSMO thin films deposited on DyScO<sub>3</sub> (DSO) substrate evidences a new phase at low temperature with dramatic anisotropic transport properties [Figs. 9(c), 9(d), and 9(e)].<sup>[158]</sup> The new phase shows preferred occupancy of the Mn 3d<sub>x<sup>2</sup>-y<sup>2</sup></sub> orbital at low temperature, which is consistent with the theoretically predicted A-type AFM phase [Fig. 9(a)].<sup>[165]</sup> However, abnormal in-plane transport anisotropy is observed in this low-temperature phase [Figs. 9(b) and 9(c)]. Note that only the film on DSO under large tensile strain shows pronounced resistivity anisotropy [Fig. 9(d)]. A switching of anisotropy sign from negative to positive upon cooling is also observed. The observed anisotropy is suggested to be driven by the preferred occupancy of the O 2p<sub>x</sub> orbitals, which hybridize with Mn 3d orbitals.

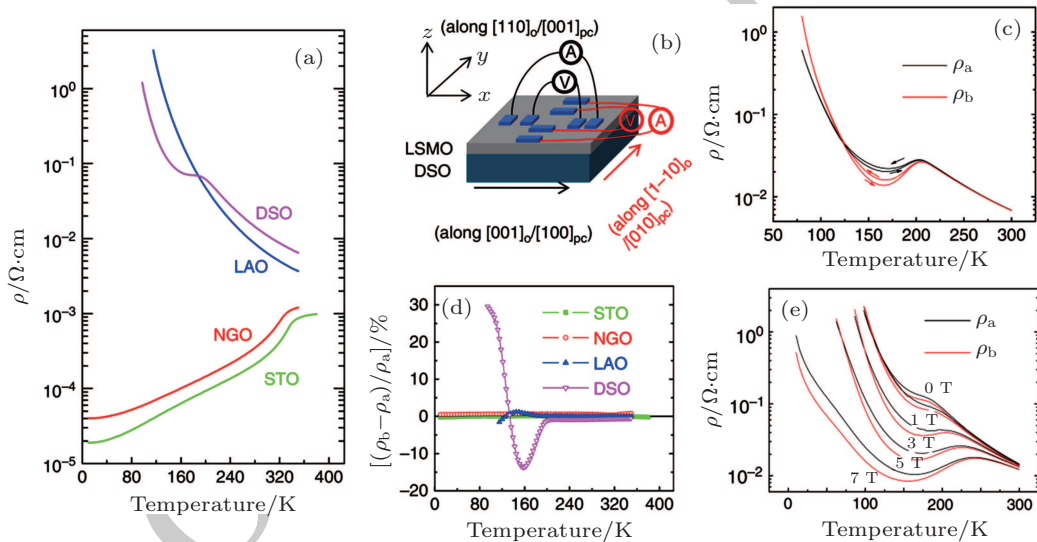


**Fig. 9.** (a) Temperature dependence of resistivity of 8-nm LSMO thin films on different substrates under zero magnetic field. (b) Schematic diagram of the experimental set-up used to measure the in-plane resistivity of the LSMO thin films along the two orthogonal directions ( $x$  and  $y$ ). (c) Resistivity versus temperature curves for 9.6-nm LSMO on DSO along the two channels during cooling and heating processes. (d) The in-plane resistivity anisotropy,  $(\rho_b - \rho_a)/\rho_a$ , of 8-nm LSMO thin films on different substrates. (e) The resistivity versus temperature curves under different magnetic fields for 9.6-nm LSMO films on DSO.<sup>[158]</sup>

### 3.2. Strain control of ferroelectric domain structures

In ferroelectric materials, the formation of ferroelectric domain structures is a consequence of minimizing the elastic and electrostatic energy of the ferroelectric system. Hence applying strain can effectively tune the ferroelectric domain structures, which could be useful for further exploring the ME properties in multiferroic systems. Both theoretical and experimental studies have been performed on controlling the ferroelectric domain structures of BFO thin films, and strain constraints have been found to be an effective way of controlling the domain structures of BFO thin films. Zhang *et al.*<sup>[40]</sup> have been trying to understand how the strain state can affect the polarization variants and to predict the domain structures in epitaxial BFO thin films with different orientations.

Their findings suggest that the domain structures of BFO thin films can be controlled by selecting the proper film orientations and strain constraints. Chu *et al.*<sup>[174]</sup> have demonstrated the realization of one-dimensional nanoscale arrays of domain walls in epitaxial BFO/SrRuO<sub>3</sub> (SRO)/DSO structures. This quasi-periodic structure results from the strain induced by the anisotropic in-plane lattice parameters of DSO ( $a_1 = 3.951 \text{ \AA}$  and  $a_2 = 3.946 \text{ \AA}$ ); it pins the structure of the SRO layer and, eventually, the ferroelectric domain structure of BFO. Through the careful control of electrostatic boundary conditions, such as the thickness of the underlying SRO layer, Chu *et al.*<sup>[175]</sup> demonstrated the creation of ordered arrays of the prototypical domain structures predicted before.<sup>[176]</sup> The selection between the 71° and 109° domain patterns depends on the electrostatic

boundary conditions, such as the existence of an SRO conducting layer and its thickness. When the bottom electrode SRO layer is thick enough to be a good metal, the elastic energy dominates the system, and the domain is fully out-of-plane polarized downward toward the SRO layer, forming ordered arrays of  $71^\circ$  domain walls. On the other hand, when the SRO layer is very thin, electrostatic energy becomes the dominant energy and the domains are alternately pointing up and down, with arrays of  $109^\circ$  domain walls favored.

Piezoelectric materials with large piezoelectric coefficients (such as lead-based perovskites PZT, PMN-PT, and PZN-PT) are typically characterized by the intimate coexistence of two phases across a morphotropic phase boundary,<sup>[177]</sup> and an electrically switching from one phase to the other.<sup>[178]</sup> By using a combination of epitaxial growth techniques in conjunction with theoretical approaches, Zeches *et al.* formed morphotropic phase boundaries through epi-

taxial constraints in lead-free piezoelectric BFO films.<sup>[41]</sup> The tetragonal-like phase can be reversibly converted into a rhombohedral-like phase, making this new lead-free system interesting for probe-based data storage and actuator applications. *Ab initio* calculations demonstrated that the strain-induced structural change in BFO [Figs. 10(a) and 10(b)] can be realized at a certain value of epitaxial strain providing the absence of misfit accommodation through dislocation formation. Direct atomic resolution images of the two phases [Figs. 10(c) and 10(d)] clearly show the difference in the crystal structures. In films grown at intermediate strain levels (e.g.,  $\sim 4.5\%$  compressive strain, corresponding to growth on  $\text{LaAlO}_3$  substrates), a nanoscale mixed-phase structure [Figs. 10(e) and 10(f)] has been observed. Figure 10(g) is an atomic resolution TEM image of the interface between these two phases and reveals one of the most provocative aspects of these structures.

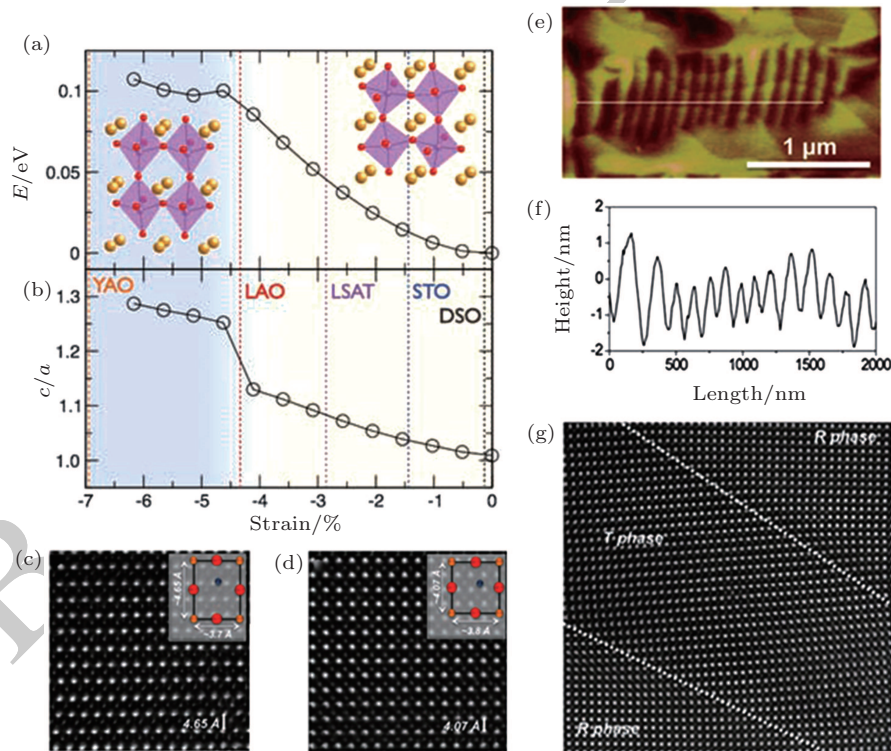


**Fig. 10.** First-principles calculations provide information on the strain evolution of (a) the overall energy of the system and (b) the  $c/a$  lattice parameter ratio. High-resolution transmission electron microscopy (HRTEM) reveals the presence of two phases (c) a highly distorted monoclinic version of a tetragonal structure and a monoclinic version of the bulk rhombohedral phase (d). These complex phase boundaries manifest themselves on the surface of the sample as imaged via (e) atomic force microscopy and these features correspond to dramatic surface height changes as shown from (f) the line trace. (g) HRTEM imaging of boundaries shows a smooth transition between phases.<sup>[41]</sup>

### 3.3. Strain mediated electrical control over magnetism

A number of works have been devoted to the study of composite multiferroic films,<sup>[96,179,180]</sup> most of which are composed of ferroelectrics and magnetic materials with layered heterostructures. In these composite multiferroic films, changes in magnetic anisotropy and coercivity can be realized by applying a strain<sup>[181,182]</sup> caused by applying an electric

field to the piezoelectric layer. Strain-mediated electric field control of magnetism has been observed in a number of epitaxial heterostructures, such as ferromagnetic LSMO films,<sup>[183]</sup> ferromagnetic CFO films<sup>[184]</sup> and metals grown on PMN-PT single crystal substrate, and ferromagnetic LSMO films<sup>[95]</sup> and metals<sup>[185]</sup> grown on BTO substrate. A giant electrical-field-induced magnetic anisotropy has been observed in these



layered multiferroic heterostructures, and the strong ME coupling is used to control the orientation of magnetization and thus enable dynamically tuning magnetoresistance in giant magnetoresistance (GMR) and anisotropic magnetoresistance (AMR) devices.<sup>[186,187]</sup>

In most cases of strain mediated electrical control over magnetism, the  $M$ - $E$  loop is butterfly-shaped, tracking the butterfly-shaped piezo-strain curve of the ferroelectric substrate, which clearly demonstrates the vital role of the elastic strains for the converse ME response in the heterostructure. For the application of information storage, tunable and non-volatile converse  $ME$  effects are two important requirements; hence loop-like behavior of the magnetic response to electric field is desirable. Therefore great efforts have been devoted to non-volatile control over magnetism.<sup>[88,188–192]</sup> For ferroelectric materials with compositions near the morphotropic phase boundary, the electric-field-induced phase transitions are very prominent. For example, a rhombohedral-to-orthorhombic phase transition takes place in (011)-oriented PZN(6-7%)-PT under sufficient poling fields. Most of such phase transitions are non-volatile, and it is expected to display a hysteresis-type lattice change as a function of electric field. This effect can

be used for realizing non-volatile spintronics and microwave devices based on multiferroic heterostructures.<sup>[180,190]</sup>

Yang *et al.* reported piezostain-mediated nonvolatile rotations of the magnetic easy axis (MEA) in the Co/PMN-PT multiferroic heterostructure at room temperature.<sup>[193]</sup> They found a reversible and non-volatile  $90^\circ$  rotation of magnetization [Fig. 11A(b) to 11A(j)], which was induced by the asymmetric butterfly-like piezostain-electric field loop for PMN-PT [Fig. 11A(a)], as has been understood by means of phase-field simulations [Fig. 11B (stage 1 and 2)]. Unexpectedly, a non-volatile  $180^\circ$  magnetization reversal is achieved without an applied magnetic field [Fig. 11B (stage 3)], and this unexpected  $180^\circ$  magnetization reversal, as is shown by phase field simulation, is mediated by simultaneous action of the piezostain and the perturbation field  $H_{\text{per}}$  that is induced by the polarization switching current. A reversible  $180^\circ$  magnetization reversal can also be realized with an auxiliary magnetic field of about 5 Oe (1 Oe =  $79.5775 \text{ A}\cdot\text{m}^{-1}$ ) [Fig. 11B, from stage 4 to stage 1]. Their discovery of the electric field-induced non-volatile, repeatable magnetization rotation could be helpful in designing electromagnetic devices.

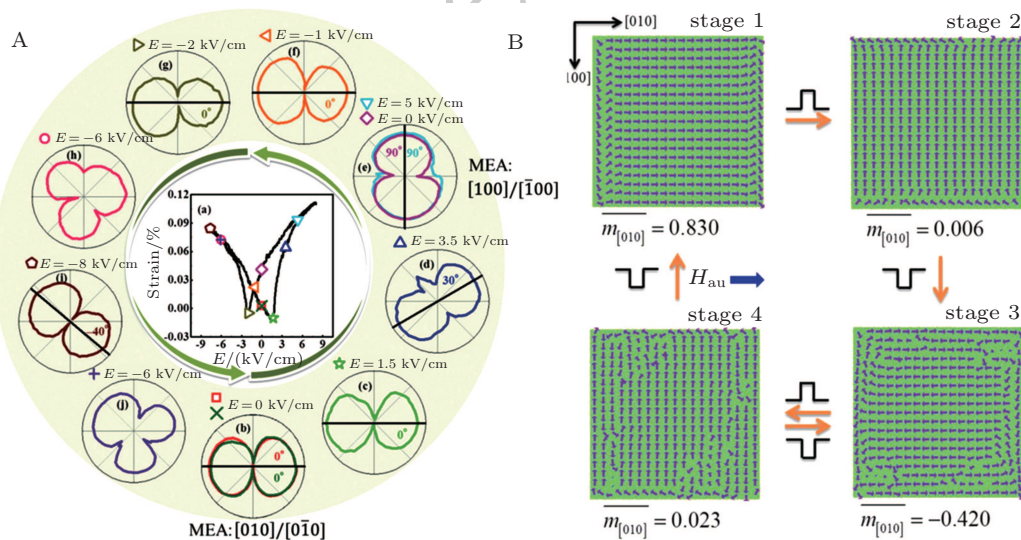


**Fig. 11.** A: (a) In-plane strain ( $\epsilon_{11}$ )–electric field loop along the [100] direction of PMN-PT. (b)–(j) The rotation history of the MEA in the Co film with a sequence of electric fields (labeled by corresponding symbols on the strain curve) applied to PMN-PT along the [100] direction in order from panel (b) to panel (j). In panel (e), after the field of  $5 \text{ kV}\cdot\text{cm}^{-1}$  is switched off, the MEA does not go back to  $0^\circ$  but remains at  $90^\circ$ . B: The magnetization domain at stages 1–4 under a stimuli sequence of  $\pm 5 \text{ kV}\cdot\text{cm}^{-1}$  (up and down pulses denoting respectively  $+5 \text{ kV}\cdot\text{cm}^{-1}$  and  $-5 \text{ kV}\cdot\text{cm}^{-1}$ ) accompanied by the  $H_{\text{per}}$  of 2 Oe induced by the polarization switching current. An auxiliary field  $H_{\text{au}}$  is used to return the magnetization to stage 1 from stage 4.<sup>[193]</sup>

Another way of realizing non-volatile electric-field-controlled magnetization is by inducing two different remnant strain states in the single-crystal piezoelectric substrate.<sup>[194]</sup> However, such an approach is not practical for real applications, as the remnant strain states strongly depend on the history of applied electric fields.

In the (001)-oriented PMN-PT substrate, a bipolar loop-like non-volatile strain has been reported, and this is ascribed

to the ferroelastic domain switching that provides a third way for realizing the non-volatile strain state.<sup>[87,88]</sup> Although much remains to be done to attain precise control of the ferroelastic domain switching process, the non-volatile strain associated with it has been proven to be promising for realizing the non-volatile control over magnetism. For example, Zhang and co-authors<sup>[195]</sup> reported a large and nonvolatile bipolar electric-field-controlled magnetization in  $\text{Co}_{40}\text{Fe}_{40}\text{B}_{20}$

on a (001)-oriented PMN-PT structure [Fig. 12(a)], which exhibits an electric-field-controlled loop-like magnetization [Figs. 12(b) and 12(c)]. This effect is related to the combined action of  $109^\circ$  ferroelastic domain switching and the absence of magnetocrystalline anisotropy in  $\text{Co}_{40}\text{Fe}_{40}\text{B}_{20}$ . The large and nonvolatile magnetoelectric coupling achieved at room temperature [Fig. 12(d)] is of great importance to achieve electric-controlled magnetic random access memories. For  $\text{Co}_{60}\text{Fe}_{20}\text{B}_{20}$  deposited on (011)-oriented PMN-PT, Liu *et al.*<sup>[189]</sup> reported up to 90% ferroelastic switching of the polarization, corresponding to rotation from an out-of-plane to a purely in-plane direction ( $71^\circ$  and  $109^\circ$  switching). The highly efficient ferroelastic switching produces two distinct, stable and electrically-reversible lattice strain states, a phenomenon that has been demonstrated to result in a highly energy-efficient, nonvolatile tuning of FMR frequency up to 2.3 GHz in elastically coupled amorphous  $\text{Co}_{60}\text{Fe}_{20}\text{B}_{20}$  films.

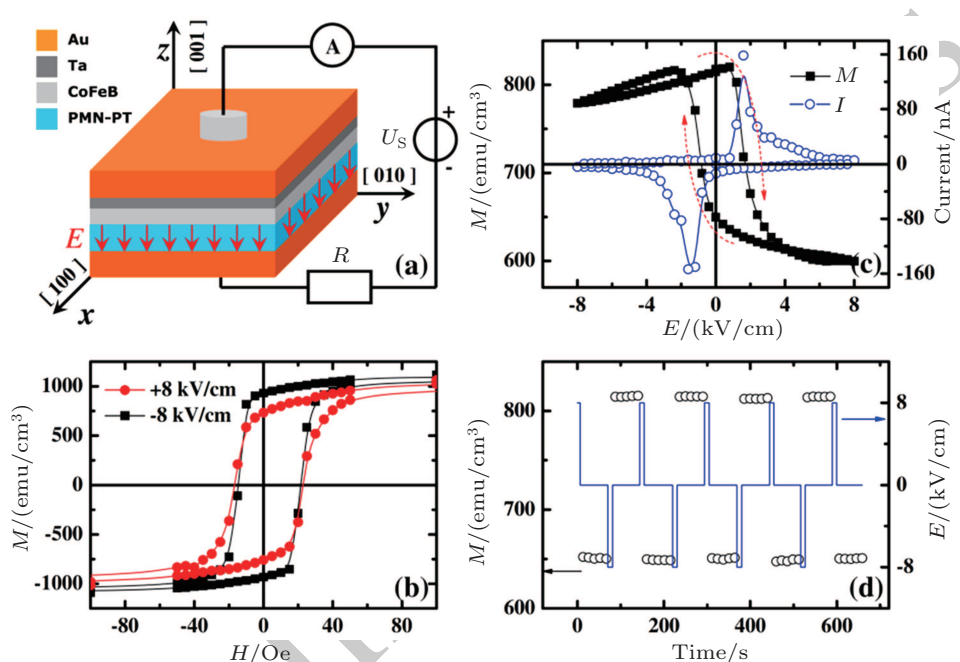


**Fig. 12.** (a) Scheme of the sample and experimental configuration. (b) In-plane magnetic hysteresis loops under electric fields of  $+8 \text{ kV}\cdot\text{cm}^{-1}$  (circle) and  $-8 \text{ kV}\cdot\text{cm}^{-1}$  (square). (c) Electric-field tuning of the in-plane magnetization (square) and polarization current (open circle) recorded at the same time. (d) The repeatable high/low magnetization states (open circle) switched by pulsed electric field (blue line).<sup>[195]</sup>

### 3.4. Flexible electronic devices

In recent years, flexible electronic devices, which offer advantages of being lightweight, foldable, and stretchable, has attracted special attention. Although a great many flexible electronic devices were made of organic materials, there has been an increasing trend in the exploration of flexible inorganic devices, such as thin-film transistors,<sup>[196–199]</sup> magnetoelectronics,<sup>[164,200,201]</sup> and memories.<sup>[202–205]</sup> In this part, we merely review the progress on flexible RRAM devices based on oxides.

In RRAM devices, the RS is dominated by the formation and rupture of the CF, as the CF is of small size and perpendicular to the film plane; hence the RS phenomenon can endure moderate strain along the film plane. There have been some reports of flexible memristive memories with a simple cross-point-type array based on various oxides such as  $\text{GeO}_x/\text{HfON}$ ,<sup>[206]</sup> aluminum oxide,<sup>[207]</sup> zinc oxide,<sup>[202,208]</sup> and  $\text{TiO}_2$ .<sup>[209,210]</sup> These devices show good flexibility, and the performance of RS is not degraded by substrate bending. In order to overcome the cell-to-cell interference issue,

Kim *et al.* developed the “NOR” type flexible RRAM with a one transistor-one memristor structure, and performed the first demonstration of random access memory operation of the RRAM on a flexible substrate.<sup>[211]</sup> Their device exhibited reliable and reproducible RS, good endurance and retention properties, along with excellent mechanical stability upon harsh bending. Liang *et al.* has demonstrated ultrathin  $\text{WO}_3\cdot\text{H}_2\text{O}$  nanosheets as a promising material to construct a high performance and flexible RRAM device [Fig. 13(a)].<sup>[212]</sup> The ultrathin  $\text{WO}_3\cdot\text{H}_2\text{O}$  nanosheets were exfoliated from the bulk hydrated tungsten oxides ( $\text{WO}_3\cdot n\text{H}_2\text{O}$ ) through a wet chemical method. Both of them show excellent RS behavior [Fig. 13(b)]; however, the device with  $\text{WO}_3\cdot\text{H}_2\text{O}$  nanosheets is superior both to its bulk counterparts and to most of the reported typical RS inorganic materials [Fig. 13(c)], possibly due to the abundant vacancy associates in the ultrathin nanosheets. In addition, due to its 2D ultrathin morphology, this nanosheets-based RRAM device also shows excellent flexibility [Fig. 13(d)], which is difficult to obtain in either bulk or nanoparticles.

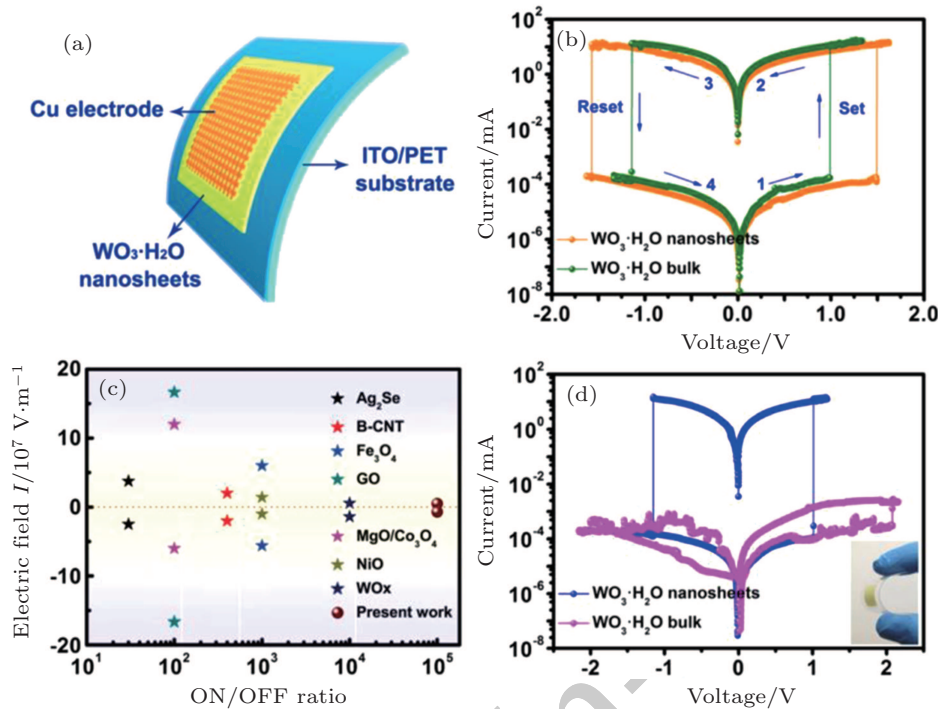


**Fig. 13.** (a) Schematic of flexible RRAM device with a Cu/WO<sub>3</sub>·H<sub>2</sub>O/ITO-PET configuration. (b) Current versus voltage ( $I$ - $V$ ) curves of the ultrathin WO<sub>3</sub>·H<sub>2</sub>O nanosheets-based and bulk-based RRAM devices at initial cycle. The arrows and numbers indicate the voltage sweep directions. (c) Comparison of the performance of the RRAM device based on ultrathin WO<sub>3</sub>·H<sub>2</sub>O nanosheets with other reported typical RS inorganic materials. (d)  $I$ - $V$  curves obtained from the WO<sub>3</sub>·H<sub>2</sub>O nanosheets-based and bulk-based RRAM devices after 2000 and 100 bending tests, respectively. Inset is a digital photograph of a bent RRAM device.<sup>[212]</sup>

## 4. Magnetic field effect

The study of magnetic field's effects on the physical properties of oxide thin films is an important issue in condensed matter physics and has shown tempting prospects of applications in spintronic devices and magnetic sensors. The discovery of the colossal magnetoresistance (CMR) effect and the investigation of all-oxide magnetic tunnel junctions (MTJ) have greatly promoted the study of magnetic field on thin film oxides. The effect of magnetic field on the electrical properties of oxide thin films has been studied in order to combine charge-tuning devices with spintronics devices.

### 4.1. Magnetoresistance effect

In perovskite manganites, applying magnetic field usually facilitates double exchange interaction which favors metallic conductivity, inducing the well-known CMR effect.<sup>[213]</sup> The CMR effect has been widely studied in manganite,<sup>[26,28,29,214–216]</sup> and it always shows a peak value near the phase boundary, which reflects the fact that the phase competition is susceptible to external magnetic field.<sup>[27]</sup> In recent years, it has been found that despite the near-cubic structure of perovskite manganites, their electron transport behavior actually depends strongly on the magnetic field direction, resulting in a very large AMR effect in manganite single crystals<sup>[217–219]</sup> and thin films.<sup>[220–224]</sup> The AMR effect shows different magnetic-field and temperature dependence

from that in 3d ferromagnetic alloys, suggesting different underlying mechanisms.<sup>[217,225,226]</sup> The AMR effect in manganite thin films can be tuned by epitaxial strain and has attracted lots of attention.<sup>[222,227–230]</sup>

### 4.2. Magnetic coupled RRAM devices

Magnetic field couples with RRAM devices in two different ways. One is by the effective tuning of the resistance switching process, and the other is by realizing more resistance states through the magnetoresistance effect. Thakare *et al.*<sup>[231]</sup> reported a bipolar RRAM of CFO/LSMO that can be gated with high sensitivity by low magnetic fields. The switching shows a strong CFO thickness-dependence only under applied magnetic field, suggesting an effective coupling with the interfacial magnetoresistive LSMO layer. Li *et al.* demonstrated three-state RS in films combining a multiferroic CFO/PZT bilayer with a semiconducting ZnO layer.<sup>[232]</sup> The three states are distinguished by various stimuli combinations of electric voltage pulse and magnetic bias, and are attributed to changes in the charge carrier states modulated by magnetoelectric coupling between CFO and PZT layers, as well as interface polarization coupling between PZT and ZnO layers. In an Si-SiO<sub>2</sub>-MgO device, the nonvolatile RS effect can be controlled by applying a magnetic field.<sup>[233]</sup> The magnetic field delays the transition from HRS to LRS and can even suppress this transition. Das *et al.*<sup>[234]</sup> observed sharp switching between low and high conducting states having a large ratio of currents

( $\sim 10^7$ ) in NiO film. Besides the switching effect, an extraordinarily large magnetoconductance ( $\sim 98\%$  at 20 K) has been found in the device, signifying multifunctional applications.

The RS effect can be utilized as a simple and controllable way to produce nanoscale devices, such as an artificial MTJ.<sup>[235]</sup> The spin transport in memristive devices has also been reported in a number of MTJs,<sup>[236–239]</sup> it is found that applying an electric field may reversibly induce two stable resistance states, respectively, with a substantial magnetoresistance difference. Li *et al.* reported the use of composite barrier layers of CoO–ZnO to fabricate the spin memris-

tive Co/CoO–ZnO/Co MTJ.<sup>[240]</sup> They found a high bipolar resistance switching ratio, up to 90 [Fig. 14(a)], and the tunnel magnetoresistance (TMR) ratio of the high resistance state reaches 8% at room temperature [Fig. 14(b)]. At the low resistance state, the TMR ratio vanishes [inset of Fig. 14(b)]. The bipolar resistance switching is attributed to the MIT of the CoO<sub>1-x</sub> layer, due to the migration of oxygen ions between CoO<sub>1-x</sub> and ZnO<sub>1-x</sub> [Fig. 14(c)]. These novel phenomena enable integrating different functionalities into a single device, which has potential applications that include multi-state storage devices and logic circuits.<sup>[239]</sup>

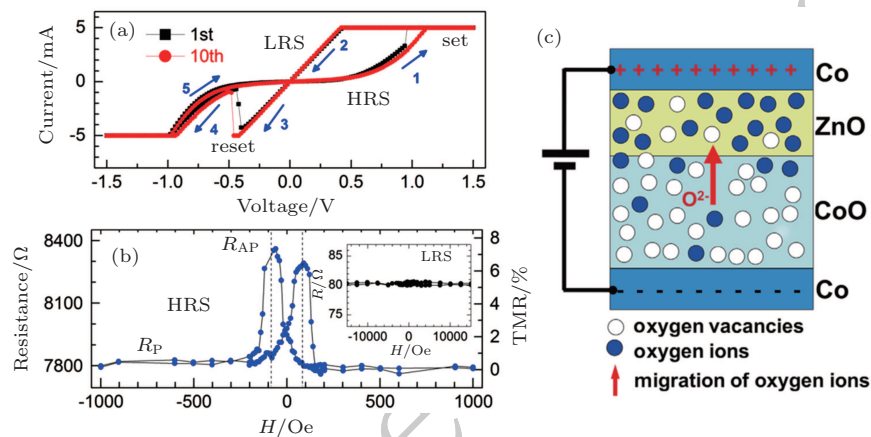


**Fig. 14.** (a) The  $I$ - $V$  characteristic of an Ag(30 nm)/Co(10 nm)/CoO–ZnO(2 nm)/Co(30 nm)/Ag(60 nm) junction with area 0.1 mm<sup>2</sup>, and (b) the tunneling magnetoresistance of the junction. The inset in panel (b) shows the  $R$ - $H$  curve of the low resistance state. Schematics of the migration of oxygen ions between very thin CoO and ZnO layers under a positive voltage, and the resulting MIT of CoO<sub>1-x</sub> in Co/CoO–ZnO/Co junctions.<sup>[240]</sup>

### 4.3. Magnetoelectric and magnetocapacitance effects

As mentioned above, the interplay between electric polarization and magnetization in multiferroic materials is very important for both fundamental physics and spintronic devices. Manipulation of magnetism by electric polarization has been demonstrated in both single-phase multiferroics and composites. Conversely, the possibility of electric polarization reversal induced by magnetic fields has been reported in multiferroics. Keeney *et al.* demonstrated switching of ferroelectric polarization by magnetic fields at room temperature in multiferroic Aurivillius phase thin films.<sup>[241]</sup> For practical applications, the weak ME coupling in single-phase multiferroics is always a big challenge.<sup>[242]</sup> Lu *et al.* reported a remarkable magnetically induced electric polarization in DyMnO<sub>3</sub> thin films, and they found an enhancement of electric polarization up to 800% upon 2 Tesla at 2 K.<sup>[42]</sup>

An efficient coupling between magnetism and dielectric properties results in phenomena such as the magnetocapacitance effect. This phenomenon has been studied in both single phase materials<sup>[47,243–247]</sup> and composite systems.<sup>[248–251]</sup> For example, the magnetocapacitance effect has been found in perovskite heterostructures such as LCMO/BTO<sup>[248]</sup> and LCMO/Ba<sub>1-x</sub>Sr<sub>x</sub>TiO<sub>3</sub><sup>[252]</sup> superlattices, manifesting an effec-

tive ME coupling in these structures. Colossal magnetocapacitance has been reported in electronic phase-separated manganite thin films, and the competition of microscopic ferromagnetic metallic and charge ordered insulating clusters is believed to play a major role in the exhibited colossal magnetocapacitance effect.<sup>[246]</sup>

## 5. Photoinduced effect

Photo-coupled phenomena have attracted wide interest due to the special advantages of light, such as high speed, low power consumption and “green” energy. In thin film oxides, photoinduced effects such as photostrictive effect,<sup>[77]</sup> photoinduced electronic phase transition,<sup>[253]</sup> photovoltaic effect<sup>[254]</sup> and photoinduced spin dynamics<sup>[255]</sup> indicate a diversity of degrees of freedom that couples effectively with light.

### 5.1. Photo-coupled RRAM devices

Light-controlled RS memory has photon-charge dual function. The resistance state can be modified not only by voltage pulses, but also by means of light. Ungureanu *et al.*<sup>[256]</sup> reported a new type of RS memory device with a simple metal/Al<sub>2</sub>O<sub>3</sub>/SiO<sub>2</sub>/Si structure. In verifying the performance of the devices when used as core of a binary memory cell, they

observed that data can be accurately written, read, and erased only under illumination [Fig. 15B] by applying 5 ms voltage pulses in the sequence  $-10\text{ V}/+6\text{ V}/+10\text{ V}/+6\text{ V}$  both in dark conditions, as well as under illumination with UV (390 nm) and IR (950 nm) light emitting diodes (LED) with irradiances up to  $2.5\text{ mW/cm}^2$ .

The change in the remnant current was interpreted as a modulation of the trapped electrons in the  $\text{Al}_2\text{O}_3$  layer. Upon the introduction of electrons from the Si layer, the resistivity of this charge storage layer increases. For positive bias, a depletion region is generated in Si at the interface with the  $\text{SiO}_2/\text{Al}_2\text{O}_3$ . The photogenerated electrons are injected into the  $\text{Al}_2\text{O}_3$  layer when the electric field is high enough to overcome this energy barrier [Fig. 15A 1, 2, and 3]. At negative voltages, the charge will be removed gradually [Fig. 15A 4, 5, and 6]. When the device is measured in dark conditions, the modulation in the remnant current is strongly suppressed, since the source of electrons is only the small dark current [Fig. 15A(a)]. The memory devices were tested and support more than  $10^4$  write/read/erase/read cycles, with a data retention time, obtained by extrapolation, of about one year. Moreover, Light-Controlled RS behavior has also been found in ZnO NRs/Nb:STO single crystal diodes<sup>[257]</sup> and ITO/ZnO

NR/Au junctions.<sup>[258]</sup>

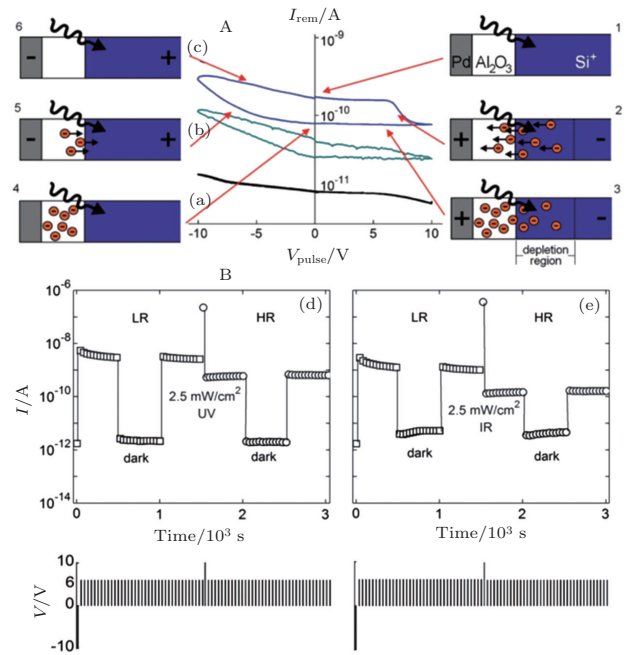


**Fig. 15.** A: Remnant current hysteresis switching loops. The measurement was taken under different UV illumination conditions. For the  $2.5\text{-mW/cm}^2$  irradiance case, the behavior was attributed to the trapped charges. B: Data retention capability in dark conditions and under illumination with UV light (a), and IR light (b) in a metal/ $\text{Al}_2\text{O}_3$ / $\text{SiO}_2$ /Si structure. The voltage-pulses applied are displayed in the lower part of the figures.<sup>[256]</sup>

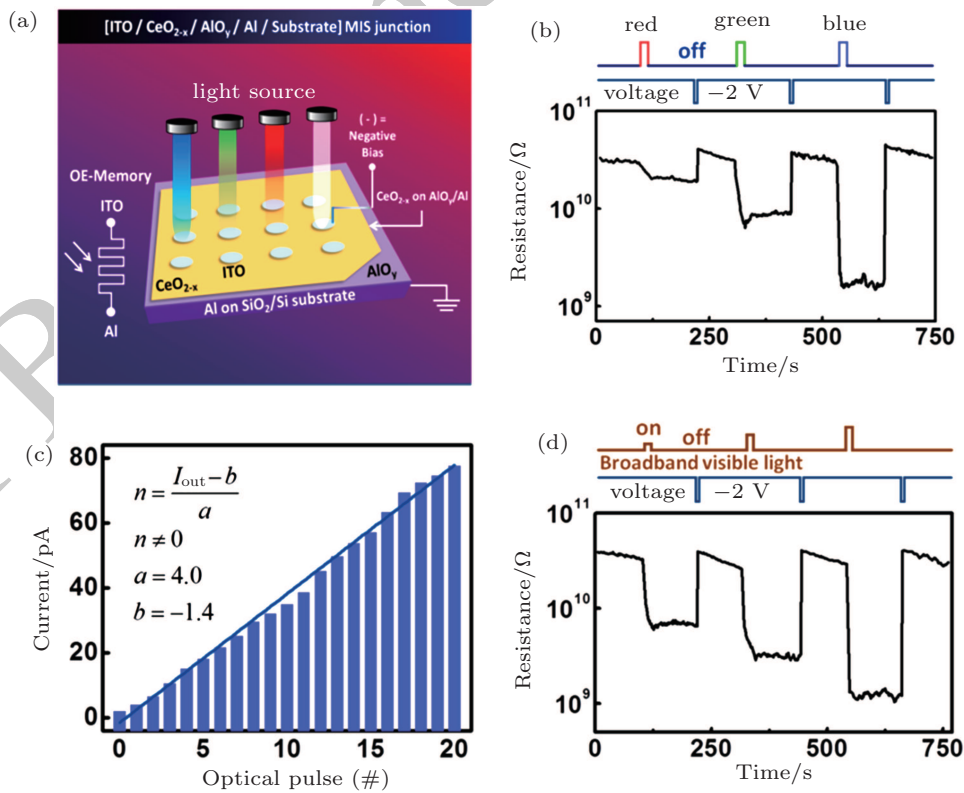


**Fig. 16.** (a) Schematic diagram of the ITO/ $\text{CeO}_{2-x}$ / $\text{AlO}_y$ /Al junction structure and the operating principle of a multifunctional optoelectronic RS memory (OE-Memory). (b) Wavelength-dependent photoresponse of the device upon being exposed to monochromatic illumination with the wavelength of 638 nm, 560 nm or 499 nm at the same intensity of  $6\text{ pW}/\mu\text{m}^2$ , respectively, enables the device as a optoelectronic demodulator. (c) Stepwise and linear relationship between the device output current and the number of the input light pulses, which forms the basis for applications of computing functions. The read voltage is  $0.1\text{ V}$ .  $I_{\text{out}}$ ,  $n$ ,  $a$ , and  $b$  stand for the output current (pA) of the device, number of light pulse inputs, photocurrent ramping step of  $\sim 4.0$  (pA) per light illumination, and a constant of  $\sim -1.4$  (pA), respectively, for  $n \neq 0$ . The dark current is  $\sim 2\text{ pA}$  for  $n = 0$ . (d) Intensity-dependent photoresponse of the device under broadband illumination with the intensities of  $8\text{ pW}/\mu\text{m}^2$ ,  $21\text{ pW}/\mu\text{m}^2$ , and  $60\text{ pW}/\mu\text{m}^2$ , respectively, renders promising multilevel storage capabilities.<sup>[259]</sup>

Recently, a multifunctional optoelectronic RS memory has been demonstrated in a simple ITO/CeO<sub>2-x</sub>/AlO<sub>y</sub>/Al structure [Fig. 16(a)].<sup>[259]</sup> As a result of the photo-induced detrapping, electrode-injection and retrapping of electrons in the CeO<sub>2-x</sub>/AlO<sub>y</sub>/Al interfacial region, the device can be optically programmed and electrically erased. The device shows broad-band, linear and persistent photoresponse, which has been utilized in integration of the demodulating [Fig. 16(b)], arithmetic [Fig. 16(c)] and memory [Fig. 16(d)] functions in a single device. This multi-functional device could be useful for future optoelectronic interconnect systems.

## 5.2. Photoinduced phase transitions

Photoinduced phase transitions have attracted special interest because they can change the properties of complex materials on the ultrafast timescale.<sup>[260–263]</sup> In perovskite manganites, photoinduced insulator-to-metal transition has been frequently reported.<sup>[264–269]</sup> Photo illumination has been found to couple coherently in these materials, resulting in modifications of a variety of the physical properties due to the strong coupling between spin, charge, orbital and lattice. In PC-SMO thin films, both photoinduced metal-to-insulator transition and photoinduced insulator-to-metal transition, have been confirmed.<sup>[270]</sup> This is a demonstration of photons as an effective way to overcome the large potential barrier due to the long-range elastic energy between the insulator and metallic phase. Possibly due to the high energies associated with photons, the photoinduced state can differ greatly from states produced with stimuli close to equilibrium. For example, in a charge-orbital ordered Nd<sub>0.5</sub>Sr<sub>0.5</sub>MnO<sub>3</sub> thin film, the photoinduced state was found to be a structurally ordered, homogeneous, metastable insulating state with crystallographic parameters different from any thermodynamically accessible state.<sup>[271]</sup>

In vanadium dioxide (VO<sub>2</sub>), a first-order transition between a high-temperature metallic phase and a low-temperature semiconducting phase has been observed.<sup>[130]</sup> A non-thermally driven ultrafast phase transition can be achieved under photo illumination.<sup>[272]</sup> The transition takes place near room temperature and has been heavily studied for both fundamental physics and possible applications such as switching devices.<sup>[58,273]</sup> There has been hot debate regarding the driving force of this insulator-metal transition, and contributions of both electron-lattice interactions and electron-electron interactions have been proposed.<sup>[274,275]</sup> Advanced time-resolved methods have been developed to capture the phase transition processes, and much has been learned about the details during the transition processes.<sup>[275,276]</sup> For instance, Morrison *et al.* utilized ultrafast electron diffraction to monitor the crystal structure of VO<sub>2</sub> and simultaneously measured its optical properties to monitor the electronic state, and they

found an interesting metastable state that preserves the initial semiconducting crystal structure while showing metal-like properties.<sup>[276]</sup>

## 5.3. Photovoltaic effect in ferroelectric thin films

Another important consequence of photo illumination is the photovoltaic effect, which has been frequently studied in ferroelectric thin films. Ferroelectric–photovoltaic devices in which a homogeneous ferroelectric material is used as a light absorbing layer have been investigated with numerous ferroelectric oxides.<sup>[277–279]</sup> The ferroelectric–photovoltaic effect is distinctly different from the typical photovoltaic effect in semiconductor p–n junctions in that the polarization electric field is the driving force for the photocurrent in ferroelectric–photovoltaic devices.<sup>[280,281]</sup> In addition, the anomalous photovoltaic effect, in which the voltage output along the polarization direction can be significantly larger than the bandgap of the ferroelectric materials, has been frequently observed in ferroelectric–photovoltaic devices.<sup>[254,282]</sup> For most ferroelectric materials, the relatively wide band gap limits photovoltaic efficiency, and utilization of narrow-band-gap ferroelectrics is therefore a promising route toward their application in both novel optoelectronic and solar energy devices.<sup>[283,284]</sup> The multiferroic material BFO, which possesses a narrow band gap ( $\sim 2.2$  eV), offers an exciting opportunity for such applications. A significant photovoltaic effect has already been observed in single crystalline BFO in both bulk<sup>[280,285,286]</sup> and thin film forms,<sup>[287–291]</sup> but it still needs improving.<sup>[254,292–294]</sup>

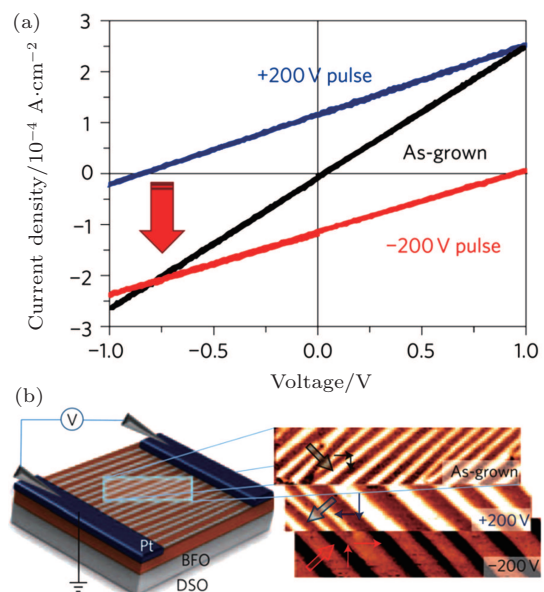


**Fig. 17.** (a) Light  $I$ - $V$  measurement in the DW<sub>||</sub> geometry shows no observable photovoltaic effect, as grown. On rotation of the domain structure to the DW<sub>⊥</sub> configuration after application of +200 V voltage pulses to the in-plane device structure, a photovoltaic effect is observed. (b) Corresponding PFM images of the as-grown (top panel), 200 V poled (middle panel), and -200 V poled (bottom panel) device structures. The arrows indicate the in-plane projection of the polarization and the net polarization direction for the entire device structure.<sup>[254]</sup>

Yang *et al.*<sup>[254]</sup> studied the photovoltaic effect on BFO film with ordered domain strips and lateral device configuration [Fig. 17(b)]. They observed that the photovoltage in the BFO film increased linearly with the total number of domain walls (DW) along the net polarization direction (perpendicular to the domain walls, poled state), and the photovoltaic effect vanished along the direction perpendicular to the net polarization direction (as-grown state) [Fig. 17(a)]. An intrinsic potential drop at domain walls ( $\sim 10$  mV), which is due to the component of the polarization perpendicular to the domain wall, induces a huge electric field of  $\sim 5 \times 10^6$  V·m<sup>-1</sup> in the narrow domain wall, which was suggested to be the driving force for the dissociation of the photo-generated exciton. The illuminated domain walls act as nanoscale photo-voltage generators connected in series, wherein the generated photocur-

rent is continuous and the photo-generated voltage accumulates along the net polarization direction.

In the ferroelectric based photovoltaic devices, it is suggested that the depolarization field may be the dominating driving force for the separation of photo-generated charge carrier-pairs. This depolarization field must be closely related to the degree of screening of the spontaneous polarization, which depends on the properties of both ferroelectric materials and electrode materials. Chen *et al.*<sup>[293]</sup> studied the anomalous photovoltaic effect in a device with a structure of Au/BFO/Au and found that the photocurrent output increased 25 times when the Au electrode was replaced by ITO. The great enhancement of photocurrent was attributed to the increased depolarizing field.

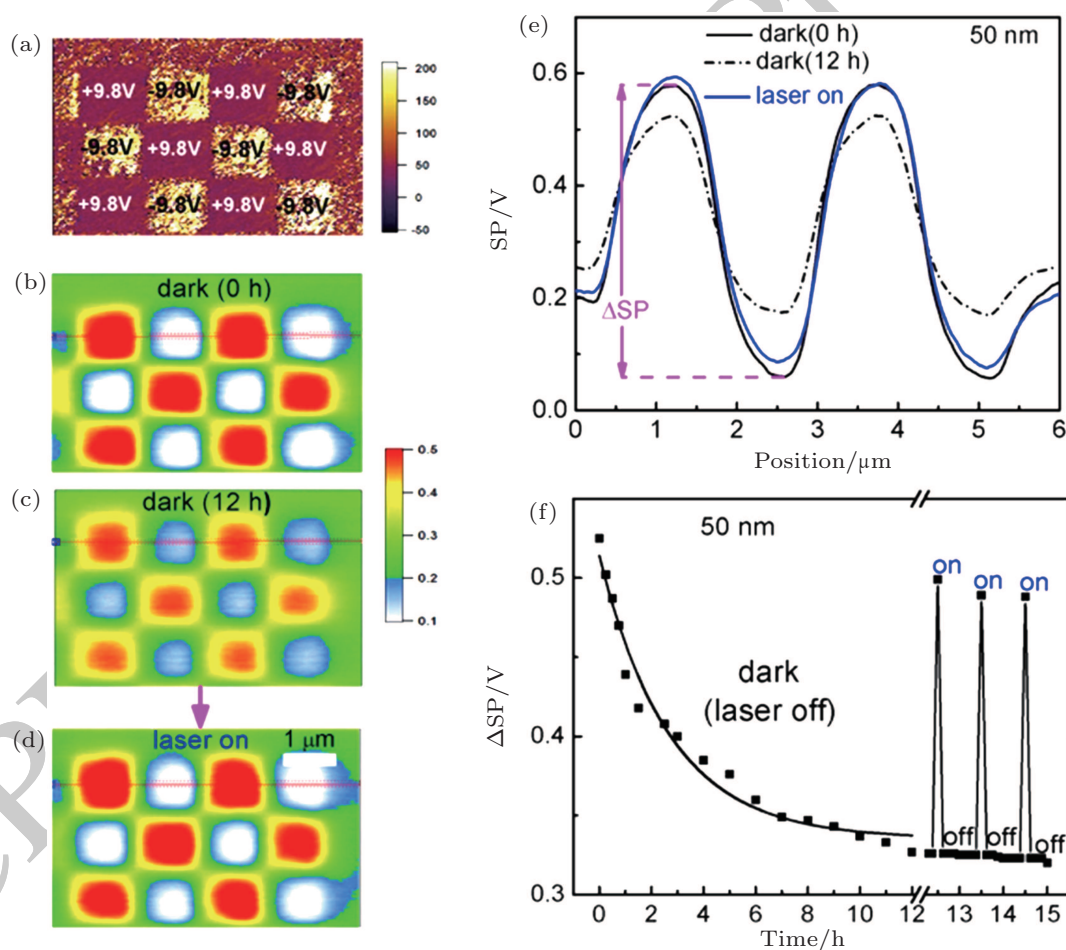


**Fig. 18.** (a) Out-of-plane PFM phase image obtained after poling for 50-nm-thick BFO films with a polarized pattern. (b)–(d) KPFM images measured without (dark) and with light illumination by a 375-nm laser (power density of  $40$  mW·cm<sup>-2</sup>). (e) Surface potential profiles obtained from panels (b)–(d), respectively. (f) Time dependence of DSP; “on” and “off” represent laser on and laser off.<sup>[296]</sup>

Furthermore, the photovoltaic effect in ferroelectric films has also provided a new method to sense the polarization direction non-destructively in ferroelectric memory. For example, Guo *et al.* reported a novel approach to create a non-volatile memory based on the ferroelectric polarization-dependent photovoltaic effect.<sup>[295]</sup> Recently, Wang *et al.* presented a new non-destructive readout by using photo-recovered surface

potential contrast.<sup>[296]</sup> By introducing laser illumination, they found that the surface potential contrast between the adjacent oppositely polarized domains can be recovered, as has been revealed by Kelvin probe force microscopy (KPFM) measurement [Figs. 18(e) and 18(f)]. The mechanism is associated with a redistribution of photoinduced charges driven by the internal electric field. They created a 12-cell memory pat-

tern based on BFO film to show the feasibility of such photo-assisted non-volatile and non-destructive readout of ferroelectric memory [Figs. 18(a)–18(d)].

## 6. Conclusions and outlook

Oxide thin films exhibit interesting and sometimes unexpected property changes upon external stimulus. These novel phenomena provide the central concept for the next generation of nanodevices. Although much progress has been made in the systems, there are still many challenges and opportunities. As an example, the emergent phenomenon at oxide interface is an interesting subject, not yet well explored.<sup>[62,66,73]</sup> In multiferroic based devices, a central idea is the electric control of magnetism that would enable scalable, green-energy spintronic devices.<sup>[297]</sup> Although the electric field induced energy-efficient control of a spin-valve device at room temperature has been demonstrated in BFO based heterostructures,<sup>[99]</sup> improving reliability of the devices is a challenge, possibly due to oxidation of the ferromagnetic metal at the interface under the strong electric field. For this reason, full study of oxide spintronics is of importance to make the device robust.<sup>[98,298]</sup> In RRAM based devices, the study of ion transport has become a new direction toward nanoscale physics, and it could be useful in designing novel electronic devices with nanoscale sizes. Difficulties lie in effective characterizations of the ionic channels, and an effective way for improving the stability and uniformity of the nanoscale devices. Given the strong composition-structure-property relationship in many complex oxides, thin film oxides show sizable and sometimes unexpected responses to external stimuli, making them a wonderful playground for studying fundamental physics and exploring novel devices. In this case, in-situ structural and chemical characterizations during film growth are desirable.

## References

- [1] Ramanathan S 2009 *Thin Film Metal-Oxides: Fundamentals and Applications in Electronics and Energy* (Springer US)
- [2] Bruce D W, O'Hare D and Walton R I 2011 *Functional Oxides* (Wiley)
- [3] Tsymbal E Y 2012 *Multifunctional Oxide Heterostructures* (OUP Oxford)
- [4] Ogale S B, Venkatesan T V and Blamire M 2013 *Functional Metal Oxides: New Science and Novel Applications* (Wiley)
- [5] Bednorz J G and Muller K A 1988 *Rev. Mod. Phys.* **60** 585
- [6] Xu Y 1991 *Ferroelectric Materials and Their Applications* (North-Holland)
- [7] Goodenough J B 2004 *Rep. Prog. Phys.* **67** 1915
- [8] Venkatesan M, Fitzgerald C B and Coey J M D 2004 *Nature* **430** 630
- [9] Izyumskaya N, Alivov Y and Morkoç H 2009 *Crit. Rev. in Solid State and Mater. Sci.* **34** 89
- [10] Dionne G F 2010 *Magnetic Oxides* (Springer US)
- [11] Lottermoser T, Lonkai T, Amann U, Hohlwein D, Ihringer J and Fiebig M 2004 *Nature* **430** 541
- [12] Bibes M and Barthelemy A 2008 *Nat. Mater.* **7** 425
- [13] Wang Z L 2010 *Nano Today* **5** 540
- [14] Yamada Y, Ueno K, Fukumura T, Yuan H T, Shimotani H, Iwasa Y, Gu L, Tsukimoto S, Ikuhara Y and Kawasaki M 2011 *Science* **332** 1065
- [15] Yu X Z, Tokunaga Y, Kaneko Y, Zhang W Z, Kimoto K, Matsui Y, Taguchi Y and Tokura Y 2014 *Nat. Commun.* **5** 3198
- [16] Kawano H, Kajimoto R, Yoshizawa H, Tomioka Y, Kuwahara H and Tokura Y 1997 *Phys. Rev. Lett.* **78** 4253
- [17] Imada M, Fujimori A and Tokura Y 1998 *Rev. Mod. Phys.* **70** 1039
- [18] Babushkina N A, Belova L M, Gorbenko O Y, Kaul A R, Bosak A A, Ozhogin V I and Kugel K I 1998 *Nature* **391** 159
- [19] Cen C, Thiel S, Hammerl G, Schneider C W, Andersen K E, Hellberg C S, Mannhart J and Levy J 2008 *Nat. Mater.* **7** 298
- [20] Scherwitzl R, Gariglio S, Gabay M, Zubko P, Gibert M and Triscone J M 2011 *Phys. Rev. Lett.* **106** 246403
- [21] Yang Z, Ko C and Ramanathan S 2011 *Ann. Rev. Mater. Res.* **41** 337
- [22] Calder S, Garlea V O, McMorro D F, Lumsden M D, Stone M B, Lang J C, Kim J W, Schlueter J A, Shi Y G, Yamaura K, Sun Y S, Tsujimoto Y and Christianson A D 2012 *Phys. Rev. Lett.* **108** 257209
- [23] Radisavljevic B and Kis A 2013 *Nat. Mater.* **12** 815
- [24] Aetukuri N B, Gray A X, Drouard M, Cossale M, Gao L, Reid A H, Kukreja R, Ohldag H, Jenkins C A, Arenholz E, Roche K P, Durr H A, Samant M G and Parkin S S P 2013 *Nat. Phys.* **9** 661
- [25] Millis A J, Shraiman B I and Mueller R 1996 *Phys. Rev. Lett.* **77** 175
- [26] Verges J A, Martin-Mayor V and Brey L 2002 *Phys. Rev. Lett.* **88** 136401
- [27] Tokura Y 2006 *Rep. Prog. Phys.* **69** 797
- [28] Uozu Y, Wakabayashi Y, Ogimoto Y, Takubo N, Tamaru H, Nagaosa N and Miyano K 2006 *Phys. Rev. Lett.* **97** 037202
- [29] Sen C, Alvarez G and Dagotto E 2010 *Phys. Rev. Lett.* **105** 097203
- [30] Sawa A 2008 *Mater. Today* **11** 28
- [31] He C L, Zhuge F, Zhou X F, Li M, Zhou G C, Liu Y W, Wang J Z, Chen B, Su W J, Liu Z P, Wu Y H, Cui P and Li R W 2009 *Appl. Phys. Lett.* **95** 232101
- [32] Yin K B, Li M, Liu Y W, He C L, Zhuge F, Chen B, Lu W, Pan X Q and Li R W 2010 *Appl. Phys. Lett.* **97** 042101
- [33] Peng S S, Zhuge F, Chen X X, Zhu X J, Hu B L, Pan L, Chen B and Li R W 2012 *Appl. Phys. Lett.* **100** 072101
- [34] Zhu X J, Shang J and Li R W 2012 *Front. Mater. Sci.* **6** 183
- [35] Zhu X J, Su W J, Liu Y W, Hu B L, Pan L, Lu W, Zhang J D and Li R W 2012 *Adv. Mater.* **24** 3941
- [36] Liu Q, Sun J, Lv H, Long S, Yin K, Wan N, Li Y, Sun L and Liu M 2012 *Adv. Mater.* **24** 1844
- [37] Shang J, Liu G, Yang H L, Zhu X J, Chen X X, Tan H W, Hu B L, Pan L, Xue W H and Li R W 2014 *Adv. Funct. Mater.* **24** 2171
- [38] Sun H, Liu Q, Li C, Long S, Lv H, Bi C, Huo Z, Li L and Liu M 2014 *Adv. Funct. Mater.* **24** 5679
- [39] Dawber M, Rabe K M and Scott J F 2005 *Rev. Mod. Phys.* **77** 1083
- [40] Zhang J X, Li Y L, Choudhury S, Chen L Q, Chu Y H, Zavaliche F, Cruz M P, Ramesh R and Jia Q X 2008 *J. Appl. Phys.* **103** 094111
- [41] Zeches R J, Rossell M D, Zhang J X, Hatt A J, He Q, Yang C H, Kumar A, Wang C H, Melville A, Adamo C, Sheng G, Chu Y H, Ihlefeld J F, Erni R, Ederer C, Gopalan V, Chen L Q, Schlom D G, Spaldin N A, Martin L W and Ramesh R 2009 *Science* **326** 977
- [42] Lu C, Dong S, Xia Z, Luo H, Yan Z, Wang H, Tian Z, Yuan S, Wu T and Liu J 2013 *Sci. Rep.* **3** 3374
- [43] Vasudevan R K, Wu W D, Guest J R, Baddorf A P, Morozovska A N, Eliseev E A, Balke N, Nagarajan V, Maksymovych P and Kalinin S V 2013 *Adv. Funct. Mater.* **23** 2592
- [44] Ren W, Yang Y, Dieguez O, Iniguez J, Choudhury N and Bellaiche L 2013 *Phys. Rev. Lett.* **110** 187601
- [45] Aoyama T, Yamauchi K, Iyama A, Picozzi S, Shimizu K and Kimura T 2014 *Nat. Commun.* **5** 4927
- [46] Hill N A 2000 *J. Phys. Chem. B* **104** 6694
- [47] Kimura T, Goto T, Shintani H, Ishizaka K, Arima T and Tokura Y 2003 *Nature* **426** 55
- [48] Eerenstein W, Mathur N D and Scott J F 2006 *Nature* **442** 759
- [49] Yamasaki Y, Miyasaka S, Kaneko Y, He J P, Arima T and Tokura Y 2006 *Phys. Rev. Lett.* **96** 207204
- [50] Hu C D 2007 *Phys. Rev. B* **75** 172106
- [51] Cheong S W and Mostovoy M 2007 *Nat. Mater.* **6** 13
- [52] Yamasaki Y, Sagayama H, Goto T, Matsuura M, Hirota K, Arima T and Tokura Y 2007 *Phys. Rev. Lett.* **98** 147204
- [53] Liu M, Obi O, Lou J, Chen Y, Cai Z, Stoute S, Espanol M, Lew M, Situ X, Ziemer K S, Harris V G and Sun N X 2009 *Adv. Funct. Mater.* **19** 1826
- [54] Kreisel J, Alexe M and Thomas P A 2012 *Nat. Mater.* **11** 260



- [55] Lee J H, Song S and Jang H M 2013 *Phys. Rev. B* **88** 014116
- [56] Cuellar F A, Liu Y H, Salafranca J, Nemes N, Iborra E, Sanchez-Santolino G, Varela M, Hernandez M G, Freeland J W, Zhernenkov M, Fitzsimmons M R, Okamoto S, Pennycook S J, Bibes M, Barthelemy A, te Velthuis S G E, Sefrioui Z, Leon C and Santamaria J 2014 *Nat. Commun.* **5** 4215
- [57] Zutic I, Fabian J and Das Sarma S 2004 *Rev. Mod. Phys.* **76** 323
- [58] Soltani M, Chaker M, Haddad E and Kruzelesky R 2006 *Meas. Sci. Tech.* **17** 1052
- [59] Scott J F 2007 *Science* **315** 954
- [60] Gajek M, Bibes M, Fusil S, Bouzehouane K, Fontcuberta J, Barthelemy A E and Fert A 2007 *Nat. Mater.* **6** 296
- [61] Meijer G I 2008 *Science* **319** 1625
- [62] Bibes M, Villegas J E and Barthelemy A 2011 *Adv. Phys.* **60** 5
- [63] Kim D J, Lu H, Ryu S, Bark C W, Eom C B, Tsymbal E Y and Gruverman A 2012 *Nano. Lett.* **12** 5697
- [64] Tokura Y and Nagaosa N 2000 *Science* **288** 462
- [65] Dagotto E and Tokura Y 2008 *MRS Bull.* **33** 1037
- [66] Hwang H Y, Iwasa Y, Kawasaki M, Keimer B, Nagaosa N and Tokura Y 2012 *Nat. Mater.* **11** 103
- [67] Yu P, Chu Y H and Ramesh R 2012 *Mater. Today* **15** 320
- [68] Kliment I K and Khomskii D I 1982 *Sov. Phys. Uspekhi* **25** 231
- [69] Watanabe H, Shirakawa T and Yunoki S 2010 *Phys. Rev. Lett.* **105** 216410
- [70] Senn M S, Wright J P and Atfield J P 2012 *Nature* **481** 173
- [71] Banerjee S, Erten O and Randeria M 2013 *Nat. Phys.* **9** 625
- [72] Gai Z, Lin W Z, Burton J D, Fuchigami K, Snijders P C, Ward T Z, Tsymbal E Y, Shen J, Jesse S, Kalinin S V and Baddorf A P 2014 *Nat. Commun.* **5** 4528
- [73] Chakhalian J, Freeland J W, Millis A J, Panagopoulos C and Rondinelli J M 2014 *Rev. Mod. Phys.* **86** 1189
- [74] Reyren N, Thiel S, Caviglia A D, Kourkoutis L F, Hammerl G, Richter C, Schneider C W, Kopp T, Rüetschi A S, Jaccard D, Gabay M, Müller D A, Triscone J M and Mannhart J 2007 *Science* **317** 1196
- [75] Mannhart J and Schlom D G 2010 *Science* **327** 1607
- [76] Jang H W, Felker D A, Bark C W, Wang Y, Niranjan M K, Nelson C T, Zhang Y, Su D, Folkman C M, Baek S H, Lee S, Janicka K, Zhu Y, Pan X Q, Fong D D, Tsymbal E Y, Rzechowski M S and Eom C B 2011 *Science* **331** 886
- [77] Kundys B, Viret M, Colson D and Kundys D O 2010 *Nat. Mater.* **9** 803
- [78] Padron-Hernandez E, Azevedo A and Rezende S M 2011 *Phys. Rev. Lett.* **107** 197203
- [79] Stiles M D and Zangwill A 2002 *Phys. Rev. B* **66** 014407
- [80] Hosomi M, Yamagishi H, Yamamoto T, Bessho K, Higo Y, Yamane K, Yamada H, Shoji M, Hachino H, Fukumoto C, Nagao H and Kano H 2005 *IEEE International Electron Devices Meeting 2005*, Technical Digest, 473
- [81] Kubota H, Fukushima A, Yakushiji K, Nagahama T, Yuasa S, Ando K, Maehara H, Nagamine Y, Tsunekawa K, Djayaprawira D D, Watanabe N and Suzuki Y 2008 *Nat. Phys.* **4** 37
- [82] Amiri P K, Zeng Z M, Upadhyaya P, Rowlands G, Zhao H, Krivorotov I N, Wang J P, Jiang H W, Katine J A, Langer J, Galatsis K and Wang K L 2011 *IEEE Electron Dev. Lett.* **32** 57
- [83] Boulle O, Cros V, Grollier J, Pereira L G, Deranlot C, Petroff F, Faini G, Barnas J and Fert A 2007 *Nat. Phys.* **3** 492
- [84] Tsymbal E Y and Kohlstedt H 2006 *Science* **313** 181
- [85] Garcia V and Bibes M 2014 *Nat. Commun.* **5** 4289
- [86] Wang C, Jin K J, Xu Z T, Wang L, Ge C, Lu H B, Guo H Z, He M and Yang G Z 2011 *Appl. Phys. Lett.* **98** 192901
- [87] Baek S H, Jang H W, Folkman C M, Li Y L, Winchester B, Zhang J X, He Q, Chu Y H, Nelson C T, Rzechowski M S, Pan X Q, Ramesh R, Chen L Q and Eom C B 2010 *Nat. Mater.* **9** 309
- [88] Yang L F, Zhao Y G, Zhang S, Li P S, Gao Y, Yang Y J, Huang H L, Miao P X, Liu Y, Chen A T, Nan C W and Gao C 2014 *Sci. Rep.* **4** 4591
- [89] Spaldin N A and Fiebig M 2005 *Science* **309** 391
- [90] Chu Y H, Martin L W, Holcomb M B, Gajek M, Han S J, He Q, Balke N, Yang C H, Lee D, Hu W, Zhan Q, Wang P L, Fraile-Rodriguez A, Scholl A, Wang S X and Ramesh R 2008 *Nat. Mater.* **7** 478
- [91] Asamitsu A, Tomioka Y, Kuwahara H and Tokura Y 1997 *Nature* **388** 50
- [92] Palanisami A, Weissman M B and Mathur N D 2005 *Phys. Rev. B* **71** 094419
- [93] Ramesh R and Spaldin N A 2007 *Nat. Mater.* **6** 21
- [94] Vaz C A F, Hoffman J, Segal Y, Marshall M S J, Reiner J W, Zhang Z, Grober R D, Walker F J and Ahn C H 2011 *J. Appl. Phys.* **109** 07D905
- [95] Eerenstein W, Wiora M, Prieto J L, Scott J F and Mathur N D 2007 *Nat. Mater.* **6** 348
- [96] Molegraaf H J A, Hoffman J, Vaz C A F, Gariglio S, van der Marel D, Ahn C H and Triscone J M 2009 *Adv. Mater.* **21** 3470
- [97] Wang J, Neaton J B, Zheng H, Nagarajan V, Ogale S B, Liu B, Viehland D, Vaithyanathan V, Schlom D G, Waghmare U V, Spaldin N A, Rabe K M, Wuttig M and Ramesh R 2003 *Science* **299** 1719
- [98] Wu S M, Cybart S A, Yu P, Rossell M D, Zhang J X, Ramesh R and Dynes R C 2010 *Nat. Mater.* **9** 756
- [99] Heron J T, Bosse J L, He Q, Gao Y, Trassin M, Ye L, Clarkson J D, Wang C, Liu J, Salahuddin S, Ralph D C, Schlom D G, Iniguez J, Huey B D and Ramesh R 2014 *Nature* **516** 370
- [100] Dzialoshinskii I E 1957 *Sov. Phys. JETP* **5** 1259
- [101] Moriya T 1960 *Phys. Rev.* **120** 91
- [102] Heron J T, Trassin M, Ashraf K, Gajek M, He Q, Yang S Y, Nikonov D E, Chu Y H, Salahuddin S and Ramesh R 2011 *Phys. Rev. Lett.* **107** 217202
- [103] Ederer C and Spaldin N A 2005 *Phys. Rev. B* **71** 060401
- [104] Beck A, Bednorz J G, Gerber C, Rossel C and Widmer D 2000 *Appl. Phys. Lett.* **77** 139
- [105] Lu W and Lieber C M 2007 *Nat. Mater.* **6** 841
- [106] Pan F, Gao S, Chen C, Song C and Zeng F 2014 *Mater. Sci. Eng.: R: Rep.* **83** 1
- [107] Jang J, Pan F, Braam K and Subramanian V 2012 *Adv. Mater.* **24** 3573
- [108] Zhu X J, Zhuge F, Li M, Yin K B, Liu Y W, Zuo Z H, Chen B and Li R W 2011 *J. Phys. D: Appl. Phys.* **44** 415104
- [109] Yan Z, Guo Y, Zhang G and Liu J M 2011 *Adv. Mater.* **23** 1351
- [110] Zhu X J, Ong C S, Xu X X, Hu B L, Shang J, Yang H L, Katlakunta S, Liu Y W, Chen X X, Pan L, Ding J and Li R W 2013 *Sci. Rep.* **3** 1084
- [111] Shang D S, Shi L, Sun J R, Shen B G, Zhuge F, Li R W and Zhao Y G 2010 *Appl. Phys. Lett.* **96** 072103
- [112] Zhuge F, Hu B L, He C L, Zhou X F, Liu Z P and Li R W 2011 *Carbon* **49** 3796
- [113] Hu B L, Zhu X J, Chen X X, Pan L, Peng S S, Wu Y Z, Shang J, Liu G, Yan Q and Li R W 2012 *J. Am. Chem. Soc.* **134** 17408
- [114] Pan L, Hu B L, Zhu X J, Chen X X, Shang J, Tan H W, Xue W H, Zhu Y J, Liu G and Li R W 2013 *J. Mater. Chem. C* **1** 4556
- [115] Jo S H and Lu W 2008 *Nano. Lett.* **8** 392
- [116] Zhuge F, Dai W, He C L, Wang A Y, Liu Y W, Li M, Wu Y H, Cui P and Li R W 2010 *Appl. Phys. Lett.* **96** 163505
- [117] Liu Q, Long S, Lv H, Wang W, Niu J, Huo Z, Chen J and Liu M 2010 *ACS Nano* **4** 6162
- [118] Long S, Perniola L, Cagli C, Buckley J, Lian X, Miranda E, Pan F, Liu M and Suñé J 2013 *Sci. Rep.* **3** 02929
- [119] Long S, Lian X, Cagli C, Cartoix'a X, Rurali R, Miranda E, Jiménez D, Perniola L, Liu M and Suñé J 2013 *Appl. Phys. Lett.* **102** 183505
- [120] Shuang G, Fei Z, Chao C, Guangsheng T, Yisong L, Zifeng Z, Cheng S and Feng P 2013 *Nanotechnology* **24** 335201
- [121] Chen C, Gao S, Zeng F, Wang G Y, Li S Z, Song C and Pan F 2013 *Appl. Phys. Lett.* **103** 043510
- [122] Syu Y E, Chang T C, Lou J H, Tsai T M, Chang K C, Tsai M J, Wang Y L, Liu M and Sze S M 2013 *Appl. Phys. Lett.* **102** 172903
- [123] Chen G, Song C, Chen C, Gao S, Zeng F and Pan F 2012 *Adv. Mater.* **24** 3515
- [124] Ren S X, Sun G W, Zhao J, Dong J Y, Wei Y, Ma Z C, Zhao X and Chen W 2014 *Appl. Phys. Lett.* **104** 232406
- [125] Ren S X, Song X T, Sun G W, Zhao X, Yang H F and Chen W 2013 *J. Mater. Chem. C* **1** 7879
- [126] Chen X X, Zhu X J, Xiao W, Liu G, Feng Y P, Ding J and Li R W 2015 *ACS Nano* **9** 4210
- [127] Gu R Y, Wang Z D and Ting C S 2003 *Phys. Rev. B* **67** 153101
- [128] Stankiewicz J, Sese J, Garcia J, Blasco J and Rillo C 2000 *Phys. Rev. B* **61** 11236
- [129] Jeon H and Biswas A 2013 *Phys. Rev. B* **88** 024415
- [130] Berglund C N and Guggenheim H J 1969 *Phys. Rev.* **185** 1022
- [131] Kim H T, Chae B G, Youn D H, Kim G, Kang K Y, Lee S J, Kim K and Lim Y S 2005 *Appl. Phys. Lett.* **86** 242101
- [132] Matsunami D and Fujita A 2015 *Appl. Phys. Lett.* **106** 042901
- [133] Driscoll T, Kim H T, Chae B G, Di Ventra M and Basov D N 2009 *Appl. Phys. Lett.* **95** 043503

- [134] Kim H T, Kim B J, Choi S, Chae B G, Lee Y W, Driscoll T, Qazilbash M M and Basov D N 2010 *J. Appl. Phys.* **107** 023702
- [135] Hyun-Tak K, Byung-Gyu C, Doo-Hyeb Y, Sung-Lyul M, Gyungock K, Kwang-Yong K and Yong-Sik L 2004 *New J. Phys.* **6** 52
- [136] Sakai J and Kurisu M 2008 *Phys. Rev. B* **78** 033106
- [137] Kumar S, Pickett M D, Strachan J P, Gibson G, Nishi Y and Williams R S 2013 *Adv. Mater.* **25** 6128
- [138] Joushaghani A, Jeong J, Paradis S, Alain D, Stewart Aitchison J and Poon J K S 2014 *Appl. Phys. Lett.* **104** 221904
- [139] Hong X, Posadas A and Ahn C H 2005 *Appl. Phys. Lett.* **86** 142501
- [140] Ahn C H, Bhattacharya A, Di Venira M, Eckstein J N, Frisbie C D, Gershenson M E, Goldman A M, Inoue I H, Mannhart J, Millis A J, Morpurgo A F, Natelson D and Triscone J M 2006 *Rev. Mod. Phys.* **78** 1185
- [141] Rondinelli J M, Stengel M and Spaldin N A 2008 *Nat. Nano* **3** 46
- [142] Niranjani M K, Velev J P, Duan C G, Jaswal S S and Tsymbal E Y 2008 *Phys. Rev. B* **78** 104405
- [143] Cai T, Ju S, Lee J, Sai N, Demkov A A, Niu Q, Li Z, Shi J and Wang E 2009 *Phys. Rev. B* **80** 140415
- [144] Niranjani M K, Burton J D, Velev J P, Jaswal S S and Tsymbal E Y 2009 *Appl. Phys. Lett.* **95** 052501
- [145] Vaz C A F, Hoffman J, Segal Y, Reiner J W, Grober R D, Zhang Z, Ahn C H and Walker F J 2010 *Phys. Rev. Lett.* **104** 127202
- [146] Vaz C A F, Segal Y, Hoffman J, Grober R D, Walker F J and Ahn C H 2010 *Appl. Phys. Lett.* **97** 042506
- [147] Hong X, Yau J B, Hoffman J D, Ahn C H, Bason Y and Klein L 2006 *Phys. Rev. B* **74** 174406
- [148] Yuan H T, Shimotani H, Tsukazaki A, Ohtomo A, Kawasaki M and Iwasa Y 2009 *Adv. Funct. Mater.* **19** 1046
- [149] Dhoot A S, Israel C, Moya X, Mathur N D and Friend R H 2009 *Phys. Rev. Lett.* **102** 136402
- [150] Hatano T, Ogimoto Y, Ogawa N, Nakano M, Ono S, Tomioka Y, Miyano K, Iwasa Y and Tokura Y 2013 *Sci. Rep.* **3** 2904
- [151] Hatano T, Sheng Z G, Nakamura M, Nakano M, Kawasaki M, Iwasa Y and Tokura Y 2014 *Adv. Mater.* **26** 2874
- [152] Nakano M, Shibuya K, Okuyama D, Hatano T, Ono S, Kawasaki M, Iwasa Y and Tokura Y 2012 *Nature* **487** 459
- [153] Jeong J, Aetukuri N, Graf T, Schladt T D, Samant M G and Parkin S S P 2013 *Science* **339** 1402
- [154] Cui B, Song C, Wang G, Yan Y, Peng J, Miao J, Mao H, Li F, Chen C, Zeng F and Pan F 2014 *Adv. Funct. Mater.* **24** 7233
- [155] Cui B, Song C, Gehring G A, Li F, Wang G, Chen C, Peng J, Mao H, Zeng F and Pan F 2014 *Adv. Funct. Mater.* **25** 864
- [156] Perroni C A, Cataudella V, De Filippis G, Iadonisi G, Ramaglia V M and Ventriglia F 2003 *Phys. Rev. B* **68** 224424
- [157] Singh S, Fitzsimmons M R, Lookman T, Jeen H, Biswas A, Roldan M A and Varela M 2012 *Phys. Rev. B* **85** 214440
- [158] Wang B M, You L, Ren P, Yin X M, Peng Y, Xia B, Wang L, Yu X J, Poh S M, Yang P, Yuan G L, Chen L, Rusydi A and Wang J L 2013 *Nat. Commun.* **4** 2778
- [159] Zheng R K, Wang Y, Chan H L W, Choy C L and Luo H S 2007 *Phys. Rev. B* **75** 212102
- [160] Rogers J A, Someya T and Huang Y 2010 *Science* **327** 1603
- [161] Lai Y C, Wang Y X, Huang Y C, Lin T Y, Hsieh Y P, Yang Y J and Chen Y F 2014 *Adv. Funct. Mater.* **24** 1430
- [162] Salvatore G A, Münzenrieder N, Kinkeldei T, Petti L, Zysset C, Strebel I, Büthe L and Tröster G 2014 *Nat. Commun.* **5** 2982
- [163] Yan C and Lee P S 2014 *Small* **10** 3443
- [164] Karnaushenko D, Makarov D, Stöber M, Karnaushenko D D, Baunack S and Schmidt O G 2015 *Adv. Mater.* **27** 880
- [165] Fang Z, Solovyev I V and Terakura K 2000 *Phys. Rev. Lett.* **84** 3169
- [166] Ahn K H, Lookman T and Bishop A R 2004 *Nature* **428** 401
- [167] Rata A D, Herklotz A, Nenkov K, Schultz L and Dorr K 2008 *Phys. Rev. Lett.* **100** 076401
- [168] Zheng R K, Habermeier H U, Chan H L W, Choy C L and Luo H S 2010 *Phys. Rev. B* **81** 104427
- [169] Zheng M, Yang M M, Zhu Q X, Li X Y, Gao G Y, Zheng R K, Wang Y, Li X M, Shi X, Luo H S and Li X G 2014 *Phys. Rev. B* **90** 224420
- [170] Heidler J, Piamonteze C, Chopdekar R V, Uribe-Laverde M A, Alberca A, Buzzi M, Uldry A, Delley B, Bernhard C and Nolting F 2015 *Phys. Rev. B* **91** 024406
- [171] Ward T Z, Budai J D, Gai Z, Tischler J Z, Yin L F and Shen J 2009 *Nat. Phys.* **5** 885
- [172] Dong S, Yunoki S, Zhang X T, Sen C, Liu J M and Dagotto E 2010 *Phys. Rev. B* **82** 035118
- [173] Mukherjee A, Cole W S, Woodward P, Randeria M and Trivedi N 2013 *Phys. Rev. Lett.* **110** 157201
- [174] Chu Y H, Zhan Q, Martin L W, Cruz M P, Yang P L, Pabst G W, Zavaliche F, Yang S Y, Zhang J X, Chen L Q, Schlom D G, Lin I N, Wu T B and Ramesh R 2006 *Adv. Mater.* **18** 2307
- [175] Chu Y H, He Q, Yang C H, Yu P, Martin L W, Shafer P and Ramesh R 2009 *Nano Lett.* **9** 1726
- [176] Streiffer S K, Parker C B, Romanov A E, Lefevre M J, Zhao L, Speck J S, Pompe W, Foster C M and Bai G R 1998 *J. Appl. Phys.* **83** 2742
- [177] Ahart M, Somayazulu M, Cohen R E, Ganesh P, Dera P, Mao H K, Hemley R J, Ren Y, Liermann P and Wu Z 2008 *Nature* **451** 545
- [178] Fu H X and Cohen R E 2000 *Nature* **403** 281
- [179] Ma J, Hu J M, Li Z and Nan C W 2011 *Adv. Mater.* **23** 1062
- [180] Liu M and Sun N X 2014 *Philos. T. R. Soc. A* **372** 20120439
- [181] Callegaro L and Puppini E 1996 *Appl. Phys. Lett.* **68** 1279
- [182] Lisfi A, Williams C M, Nguyen L T, Lodder J C, Coleman A, Corcoran H, Johnson A, Chang P, Kumar A and Morgan W 2007 *Phys. Rev. B* **76** 054405
- [183] Thiele C, Dorr K, Bilani O, Rodel J and Schultz L 2007 *Phys. Rev. B* **75** 054408
- [184] Yang J J, Zhao Y G, Tian H F, Luo L B, Zhang H Y, He Y J and Luo H S 2009 *Appl. Phys. Lett.* **94** 212504
- [185] Sahoo S, Polisetty S, Duan C G, Jaswal S S, Tsymbal E Y and Binek C 2007 *Phys. Rev. B* **76** 092108
- [186] Liu M, Obi O, Lou J, Li S D, Xing X, Yang G M and Sun N X 2011 *J. Appl. Phys.* **109** 07D913
- [187] Liu M, Li S D, Obi O, Lou J, Rand S and Sun N X 2011 *Appl. Phys. Lett.* **98** 222509
- [188] Parkes D E, Cavill S A, Hindmarch A T, Wadley P, Mcgee F, Staddon C R, Edmonds K W, Campion R P, Gallagher B L and Rushforth A W 2012 *Appl. Phys. Lett.* **101** 072402
- [189] Liu M, Howe B M, Grazulis L, Mahalingam K, Nan T X, Sun N X and Brown G J 2013 *Adv. Mater.* **25** 4886
- [190] Wang Z, Wang Y, Ge W, Li J and Viehland D 2013 *Appl. Phys. Lett.* **103** 132909
- [191] Liu M, Hoffman J, Wang J, Zhang J X, Nelson-Cheeseman B and Bhattacharya A 2013 *Sci. Rep.* **3** 1876
- [192] Zhou Z, Zhang X Y, Xie T F, Nan T X, Gao Y, Yang X, Wang X J, He X Y, Qiu P S, Sun N X and Sun D Z 2014 *Appl. Phys. Lett.* **104** 012905
- [193] Yang S W, Peng R C, Jiang T, Liu Y K, Feng L, Wang J J, Chen L Q, Li X G and Nan C W 2014 *Adv. Mater.* **26** 7091
- [194] Wu T, Bur A, Zhao P, Mohanchandra K P, Wong K, Wang K L, Lynch C S and Carman G P 2011 *Appl. Phys. Lett.* **98** 012504
- [195] Zhang S, Zhao Y G, Li P S, Yang J J, Rizwan S, Zhang J X, Seidel J, Qu T L, Yang Y J, Luo Z L, He Q, Zou T, Chen Q P, Wang J W, Yang L F, Sun Y, Wu Y Z, Xiao X, Jin X F, Huang J, Gao C, Han X F and Ramesh R 2012 *Phys. Rev. Lett.* **108** 137203
- [196] Nomura K, Ohta H, Takagi A, Kamiya T, Hirano M and Hosono H 2004 *Nature* **432** 488
- [197] Liu J, Buchholz D B, Hennek J W, Chang R P H, Facchetti A and Marks T J 2010 *J. Am. Chem. Soc.* **132** 11934
- [198] Jae Kyeong J 2011 *Semicond. Sci. Technol.* **26** 034008
- [199] Kim Y H, Heo J S, Kim T H, Park S, Yoon M H, Kim J, Oh M S, Yi G R, Noh Y Y and Park S K 2012 *Nature* **489** 128
- [200] Chen Y F, Mei Y, Kaltfofen R, Mönch J I, Schumann J, Freudenberger J, Klauß H J and Schmidt O G 2008 *Adv. Mater.* **20** 3224
- [201] Liu Y W, Zhan Q F and Li R W 2013 *Chin. Phys. B* **22** 127502
- [202] Lee S, Kim H, Yun D J, Rhee S W and Yong K 2009 *Appl. Phys. Lett.* **95** 262113
- [203] Yao J, Lin J, Dai Y, Ruan G, Yan Z, Li L, Zhong L, Natelson D and Tour J M 2012 *Nat. Commun.* **3** 1101
- [204] Han S T, Zhou Y and Roy V A L 2013 *Adv. Mater.* **25** 5425
- [205] Pan L, Ji Z H, Yi X H, Zhu X J, Chen X X, Shang J, Liu G and Li R W 2015 *Adv. Funct. Mater.*
- [206] Cheng C H, Yeh F S and Chin A 2011 *Adv. Mater.* **23** 902
- [207] Kim S and Choi Y K 2008 *Appl. Phys. Lett.* **92** 223508
- [208] Won Seo J, Park J W, Lim K S, Kang S J, Hong Y H, Yang J H, Fang L, Sung G Y and Kim H K 2009 *Appl. Phys. Lett.* **95** 133508
- [209] Yun J, Cho K, Park B, Park B H and Kim S 2009 *J. Mater. Chem.* **19** 2082

- [210] Hu Young J, Yong In K, Jeong Yong L and Sung-Yool C 2010 *Nanotechnology* **21** 115203
- [211] Kim S, Jeong H Y, Kim S K, Choi S Y and Lee K J 2011 *Nano Lett.* **11** 5438
- [212] Liang L, Li K, Xiao C, Fan S, Liu J, Zhang W, Xu W, Tong W, Liao J, Zhou Y, Ye B and Xie Y 2015 *J. Am. Chem. Soc.* **137** 3102
- [213] Jin S, Tiefel T H, McCormack M, Fastnacht R A, Ramesh R and Chen L H 1994 *Science* **264** 413
- [214] Jin S, Tiefel T H, McCormack M, Obryan H M, Chen L H, Ramesh R and Schurig D 1995 *Appl. Phys. Lett.* **67** 557
- [215] Urushibara A, Moritomo Y, Arima T, Asamitsu A, Kido G and Tokura Y 1995 *Phys. Rev. B* **51** 14103
- [216] Matl P, Ong N P, Yan Y F, Li Y Q, Studebaker D, Baum T and Doubinina G 1998 *Phys. Rev. B* **57** 10248
- [217] Li R W, Wang H B, Wang X W, Yu X Z, Matsui Y, Cheng Z H, Shen B G, Plummer E W and Zhang J D 2009 *Proc. Natl. Acad. Sci. USA* **106** 14224
- [218] Ning W, Qu Z, Zou Y M, Ling L S, Zhang L, Xi C Y, Du H F, Li R W and Zhang Y H 2011 *Appl. Phys. Lett.* **98** 212503
- [219] Yang H L, Liu Y W, Zhang J D, Zhang X Q, Cheng Z H, Xie Y L, Wang B M, Zhan Q F, Shen B G, Plummer E W and Li R W 2015 *Phys. Rev. B* accepted
- [220] Eckstein J N, Bozovic I, O'Donnell J, Onellion M and Rzczowski M S 1996 *Appl. Phys. Lett.* **69** 1312
- [221] Li Q, Wang H S, Hu Y F and Wertz E 2000 *J. Appl. Phys.* **87** 5573
- [222] Egilmez M, Saber M M, Mansour A I, Ma R, Chow K H and Jung J 2008 *Appl. Phys. Lett.* **93** 182505
- [223] Bason Y, Hoffman J, Ahn C H and Klein L 2009 *Phys. Rev. B* **79** 092406
- [224] Srivastava M K, Kaur A and Singh H K 2012 *Appl. Phys. Lett.* **100** 222408
- [225] Zhang Y Q, Meng H, Wang X W, Liu J J, Du J and Zhang Z D 2011 *Appl. Phys. Lett.* **99** 252502
- [226] Yang H, Wang B, Liu Y, Yang Z, Zhu X, Xie Y, Zuo Z, Chen B, Zhan Q, Wang J and Li R W 2014 *J. Appl. Phys.* **116** 234505
- [227] Egilmez M, Mansour A I, Saber M M, Chow K H and Jung J 2008 *Appl. Phys. Lett.* **92** 022501
- [228] Zhang F H, Huang Z, Gao G Y, Chen P F, Wang L F, Tan X L and Wu W B 2010 *Appl. Phys. Lett.* **96** 062507
- [229] Xie Y L, Yang H L, Liu Y W, Yang Z H, Chen B, Zuo Z H, Katlakunta S, Zhan Q F and Li R W 2013 *J. Appl. Phys.* **113** 17C716
- [230] Yang H, Liu Y and Li R W 2012 *SPIN* **02** 1230004
- [231] Thakare V, Xing G Z, Peng H Y, Rana A, Game O, Kumar P A, Banpurkar A, Kolekar Y, Ghosh K, Wu T, Sarma D D and Ogale S B 2012 *Appl. Phys. Lett.* **100** 172412
- [232] Li Z, Zhou M, Ding W, Zhou H, Chen B, Wan J G, Liu J M and Wang G 2012 *Appl. Phys. Lett.* **100** 262903
- [233] Wang J M, Zhang X Z, Piao H G, Luo Z C, Xiong C Y, Wang X F and Yang F H 2014 *Appl. Phys. Lett.* **104** 243511
- [234] Das S, Majumdar S and Giri S 2010 *J. Phys. Chem. C* **114** 6671
- [235] Yang Z H, Zhan Q F, Zhu X J, Liu Y W, Yang H L, Hu B L, Shang J, Pan L, Chen B and Li R W 2014 *Europhys. Lett.* **108** 58004
- [236] Bowen M, Maurice J L, Barthélemy A, Prod'homme P, Jacquet E, Contour J P, Imhoff D and Colliex C 2006 *Appl. Phys. Lett.* **89** 103517
- [237] Halley D, Majjad H, Bowen M, Najjari N, Henry Y, Ulhaq-Bouillet C, Weber W, Bertoni G, Verbeeck J and Van Tendeloo G 2008 *Appl. Phys. Lett.* **92** 212115
- [238] Jang H J, Kirillov O A, Jurchescu O D and Richter C A 2012 *Appl. Phys. Lett.* **100** 043510
- [239] Prezioso M, Riminucci A, Graziosi P, Bergenti I, Rakshit R, Cecchini R, Vianelli A, Borgatti F, Haag N, Willis M, Drew A J, Gillin W P and Dediu V A 2013 *Adv. Mater.* **25** 534
- [240] Li Q, Shen T T, Cao Y L, Zhang K, Yan S S, Tian Y F, Kang S S, Zhao M W, Dai Y Y, Chen Y X, Liu G L, Mei L M, Wang X L and Grünberg P 2014 *Sci. Rep.* **4** 03835
- [241] Keeney L, Maity T, Schmidt M, Amann A, Deepak N, Petkov N, Roy S, Pemble M E and Whatmore R W 2013 *J. Am. Ceram. Soc.* **96** 2339
- [242] Miao H C, Zhou X L, Dong S X, Luo H S and Li F X 2014 *Nanoscale* **6** 8515
- [243] Rogado N S, Li J, Sleight A W and Subramanian M A 2005 *Adv. Mater.* **17** 2225
- [244] Kimura T, Kawamoto S, Yamada I, Azuma M, Takano M and Tokura Y 2003 *Phys. Rev. B* **67** 180401
- [245] Xiang H J and Whangbo M H 2007 *Phys. Rev. Lett.* **98** 246403
- [246] Rairigh R P, Singh-Bhalla G, Tongay S, Dhakal T, Biswas A and Hebard A F 2007 *Nat. Phys.* **3** 551
- [247] Ghosh A, Dey K, Sabyasachi S, Karmakar A, Majumdar S and Giri S 2013 *Appl. Phys. Lett.* **103** 052412
- [248] Singh M P, Prellier W, Simon C and Raveau B 2005 *Appl. Phys. Lett.* **87** 022505
- [249] Parish M M and Littlewood P B 2008 *Phys. Rev. Lett.* **101** 166602
- [250] Pertsev N A, Prokhorenko S and Dkhil B 2012 *Phys. Rev. B* **85** 134111
- [251] Lee S N, Shim H J and Shim I B 2014 *J. Magn.* **19** 121
- [252] Singh M P, Prellier W, Mechin L and Raveau B 2006 *Appl. Phys. Lett.* **88** 012903
- [253] Miyano K, Tanaka T, Tomioka Y and Tokura Y 1997 *Phys. Rev. Lett.* **78** 4257
- [254] Yang S Y, Seidel J, Byrnes S J, Shafer P, Yang C H, Rossell M D, Yu P, Chu Y H, Scott J F, Ager J W, Martin L W and Ramesh R 2010 *Nat. Nano* **5** 143
- [255] Ogasawara T, Ohgushi K, Tomioka Y, Takahashi K S, Okamoto H, Kawasaki M and Tokura Y 2005 *Phys. Rev. Lett.* **94** 087202
- [256] Ungureanu M, Zazpe R, Golmar F, Stoliar P, Llopis R, Casanova F and Hueso L E 2012 *Adv. Mater.* **24** 2496
- [257] Bera A, Peng H Y, Lourembam J, Shen Y D, Sun X W and Wu T 2013 *Adv. Funct. Mater.* **23** 4977
- [258] Park J, Lee S, Lee J and Yong K 2013 *Adv. Mater.* **25** 6423
- [259] Tan H W, Liu G, Zhu X J, Yang H L, Chen B, Chen X X, Shang J, Lu W, Wu Y H and Li R W 2015 *Adv. Mater.* **27** 2797
- [260] Cavalleri A, Chong H H W, Fourmaux S, Glover T E, Heimann P A, Kieffer J C, Mun B S, Padmore H A and Schoenlein R W 2004 *Phys. Rev. B* **69** 153106
- [261] Cavalleri A, Dekorsy T, Chong H H W, Kieffer J C and Schoenlein R W 2004 *Phys. Rev. B* **70** 161102
- [262] Okimoto Y, Peng X, Tamura M, Morita T, Onda K, Ishikawa T, Koshihara S, Todoroki N, Kyomen T and Itoh M 2009 *Phys. Rev. Lett.* **103** 027402
- [263] Okamoto H, Miyagoe T, Kobayashi K, Uemura H, Nishioka H, Matsuzaki H, Sawa A and Tokura Y 2011 *Phys. Rev. B* **83** 125102
- [264] Oshima H, Miyano K, Konishi Y, Kawasaki M and Tokura Y 1999 *Appl. Phys. Lett.* **75** 1473
- [265] Sasaki M, Wu G R, Gao W X, Negishi H, Inoue M and Xiong G C 1999 *Phys. Rev. B* **59** 12425
- [266] Dai J M, Song W H, Du J J, Wang J N and Sun Y P 2003 *Phys. Rev. B* **67** 144405
- [267] Matsubara M, Okimoto Y, Ogasawara T, Tomioka Y, Okamoto H and Tokura Y 2007 *Phys. Rev. Lett.* **99** 207401
- [268] Polli D, Rini M, Wall S, Schoenlein R W, Tomioka Y, Tokura Y, Cerullo G and Cavalleri A 2007 *Nat. Mater.* **6** 643
- [269] Beaud P, Johnson S L, Vorobeve E, Staub U, De Souza R A, Milne C J, Jia Q X and Ingold G 2009 *Phys. Rev. Lett.* **103** 155702
- [270] Takubo N, Onishi I, Takubo K, Mizokawa T and Miyano K 2008 *Phys. Rev. Lett.* **101** 177403
- [271] Ichikawa H, Nozawa S, Sato T, Tomita A, Ichiyangi K, Chollet M, Guerin L, Dean N, Cavalleri A, Adachi S, Arima T, Sawa H, Ogiimoto Y, Nakamura M, Tamaki R, Miyano K and Koshihara S 2011 *Nat. Mater.* **10** 101
- [272] Becker M F, Buckman A B, Walser R M, Lépine T, Georges P and Brun A 1994 *Appl. Phys. Lett.* **65** 1507
- [273] Lee M J, Park Y, Suh D S, Lee E H, Seo S, Kim D C, Jung R, Kang B S, Ahn S E, Lee C B, Seo D H, Cha Y K, Yoo I K, Kim J S and Park B H 2007 *Adv. Mater.* **19** 3919
- [274] Haverkort M W, Hu Z, Tanaka A, Reichelt W, Streltsov S V, Korotin M A, Anisimov V I, Hsieh H H, Lin H J, Chen C T, Khomskii D I and Tjeng L H 2005 *Phys. Rev. Lett.* **95** 196404
- [275] Laverock J, Kittiwatanakul S, Zakharov A A, Niu Y R, Chen B, Wolf S A, Lu J W and Smith K E 2014 *Phys. Rev. Lett.* **113** 216402
- [276] Morrison V R, Chatelain R P, Tiwari K L, Hendaoui A, Bruhács A, Chaker M and Siwick B J 2014 *Science* **346** 445
- [277] Chen B, Zuo Z H, Liu Y W, Zhan Q F, Xie Y L, Yang H L, Dai G H, Li Z X, Xu G J and Li R W 2012 *Appl. Phys. Lett.* **100** 173903
- [278] Cao D W, Wang C Y, Zheng F G, Dong W, Fang L and Shen M R 2012 *Nano Lett.* **12** 2803

- [279] Grinberg I, West D V, Torres M, Gou G Y, Stein D M, Wu L Y, Chen G N, Gallo E M, Akbashev A R, Davies P K, Spanier J E and Rappe A M 2013 *Nature* **503** 509
- [280] Choi T, Lee S, Choi Y J, Kiryukhin V and Cheong S W 2009 *Science* **324** 63
- [281] Zhang J J, Su X D, Shen M R, Shen Z H, Zhang L J, Zhang X Y, Cheng W X, Cao M Y and Zou G 2013 *Sci. Rep.* **3** 2109
- [282] Zenkevich A, Matveyev Y, Maksimova K, Gaynutdinov R, Tolstikhina A and Fridkin V 2014 *Phys. Rev. B* **90** 161409
- [283] Yang X L, Su X D, Shen M R, Zheng F G, Xin Y, Zhang L, Hua M C, Chen Y J and Harris V G 2012 *Adv. Mater.* **24** 1202
- [284] Choi W S, Chisholm M F, Singh D J, Choi T, Jellison G E and Lee H N 2012 *Nat. Commun.* **3** 689
- [285] Moubah R, Rousseau O, Colson D, Artemenko A, Maglione M and Viret M 2012 *Adv. Funct. Mater.* **22** 4814
- [286] Alexe M 2012 *Nano Lett.* **12** 2193
- [287] Yang S Y, Martin L W, Byrnes S J, Conry T E, Basu S R, Paran D, Reichertz L, Ihlefeld J, Adamo C, Melville A, Chu Y H, Yang C H, Musfeldt J L, Schlom D G, Ager J W and Ramesh R 2009 *Appl. Phys. Lett.* **95** 062909
- [288] Qu T L, Zhao Y G, Xie D, Shi J P, Chen Q P and Ren T L 2011 *Appl. Phys. Lett.* **98** 173507
- [289] Wang L, Jin K J, Ge C, Wang C, Guo H Z, Lu H B and Yang G Z 2013 *Appl. Phys. Lett.* **102** 252907
- [290] Gao R L, Chen Y S, Sun J R, Zhao Y G, Li J B and Shen B G 2013 *J. Appl. Phys.* **113** 183510
- [291] Anshul A, Borkar H, Singh P, Pal P, Kushvaha S S and Kumar A 2014 *Appl. Phys. Lett.* **104** 132910
- [292] Alexe M and Hesse D 2011 *Nat. Commun.* **2** 256
- [293] Chen B, Li M, Liu Y W, Zuo Z H, Zhuge F, Zhan Q F and Li R W 2011 *Nanotechnology* **22** 195201
- [294] Gao R L, Yang H W, Fu C L, Cai W, Chen G, Deng X L, Sun J R, Zhao Y G and Shen B G 2015 *J. Alloys Compd.* **624** 1
- [295] Guo R, You L, Zhou Y, Shih Lim Z, Zou X, Chen L, Ramesh R and Wang J 2013 *Nat. Commun.* **4** 2990
- [296] Wang L, Jin K J, Gu J X, Ma C, He X, Zhang J, Wang C, Feng Y, Wan Q, Shi J A, Gu L, He M, Lu H B and Yang G Z 2014 *Sci. Rep.* **4** 6980
- [297] Scott J F 2007 *Nat. Mater.* **6** 256
- [298] Haghiri-Gosnet A M, Arnal T, Soulimane R, Koubaa M and Renard J P 2004 *Phys. Status Solidi A: Appl. Res.* **201** 1392